Late Holocene ecological shifts and chironomid-inferred summer temperature changes reconstructed from Lake Uddelermeer, the Netherlands

M.T.I.J. Gouw-Bouman[a] , N. van Asch[b], S. Engels[c] , W.Z. Hoek[a]

[a] *Utrecht University, Faculty of Geosciences, Dept. of Physical Geography, Princetonlaan 8A, 3584 CB, Utrecht, The Netherlands*

[b] *ADC Archeoprojecten, Nijverheidweg-Noord 114, 3812 PN Amersfoort, the Netherlands*

[c] *Birkbeck University of London, Department of Geography, 32 Tavistock Square, WC1H 9EZ, London, United Kingdom*

*Corresponding author e-mail: mtij.gouw@gmail.com

Abstract

This paper presents a Late-Holocene chironomid-inferred July-air temperature record from a core obtained from Lake Uddelermeer in the Netherlands. A core interval, which dates from 2500 to 400 cal. yr. BP, was analysed at multi-decadal resolution for organic content, pollen, spores and NPPs (Non Pollen Palynomorphs), and chironomid head capsules. These proxies indicate that, from 2500 to 1140 cal. yr. BP, the lake was mesotrophic and sustained a *Littorellion,* while the chironomid assemblage was dominated by littoral species associated with macrophytes. At 1140 cal. yr. BP a shift in the lake ecology occurred from low-nutrient to high-nutrient conditions dominated by algae. This shift might be linked to a concurrent increase in human impact and is reflected in the chironomid assemblage by increases in eurytopic taxa, which are resistant to disturbances. Shifts in the chironomid record between 2500 and 1140 cal. yr. BP do not coincide with changes in lake ecology and are presumably driven by climate change. Using a Norwegian-Swiss calibration dataset as a modern analogue, we produced a chironomid-inferred temperature (C-IT) reconstruction. This reconstruction compares well to other regional temperature reconstructions in timing and duration with a Roman Warm period between 2240-1760 cal. yr. BP, a Dark Age Cold Period starting at 1760 cal. yr. BP and the Medieval Climate Anomaly beginning at 1280 cal. yr. BP. The C-IT record indicates a temperature drop of 1.5°C from the Roman Warm Period to the Dark Age Cold Period. Findings improve knowledge of the first millennium AD in NW Europe, which was characterised by changes in landscape, vegetation, society and climate.

Keywords

first millennium AD; non-biting midges; July air temperature; Dark Age Cold Period; Roman Warm Period; North-western Europe

1 Introduction

Many studies have shown that past climate fluctuations might be temporally linked to cultural shifts (Tinner *et al.* 2003; Büntgen *et al.* 2011; McCormick *et al.* 2012a; Büntgen *et al.* 2016). During the first millennium AD two large cultural transitions occurred in NW Europe: the decline of the Roman Empire and the later transition to medieval kingdoms. Recent studies (e.g. Büntgen *et al.* 2016b; Helama *et al.* 2017a; Helama *et al.* 2017b) have shown that climate in NW Europe during the first millennium was not as stable as previously assumed or as

evidenced from global climate reconstructions (Rasmussen *et al.* 2006; Vinther *et al.* 2006; Wanner *et al.* 2008). Riechelmann and Gouw-Bouman (2019) indicate the presence of a Roman Warm Period (RWP; 1950-1700 cal. yr. BP), a Dark Age Cold Period (DACP; 1700-1250 cal. yr. BP) and a Medieval Warm Period or Medieval Climate Optimum (MCA; 1250-950 cal. yr. BP) in NW Europe (table 1). Other climate reconstructions from the Northern Hemisphere also demonstrate the occurrence of significant climatic shifts during this time interval (e.g. Larsen *et al.* 2008; Ljungqvist 2010; Wanner *et al.* 2011; Gräslund and Price 2012; McCormick *et al.* 2012b; Büntgen *et al.* 2016b; Toohey *et al.* 2016; Helama *et al.* 2017a). The identification of similar warm and cold periods in numerous proxy records throughout NW Europe indicates a regional climate trend (Helama *et al.* 2017a; Riechelmann and Gouw-Bouman 2019).

Following the collapse of the Roman Empire a decrease in population density, from approximately 1680-1450 cal. yr. BP (AD 270 to AD 500), was seen in the Netherlands, this time period is also known as the Migration Period. This was followed by an exponential population growth from 1350 cal. yr. BP (AD 600) onward when the medieval kingdoms emerged (Pierik and van Lanen 2017; Groenewoudt and van Lanen 2018; Pierik *et al.* 2018) (table 1). Not only do these cultural shifts occur contemporaneously with climatic changes, they also are concurrent with large-scale landscape and vegetation changes in the Netherlands (Jansma *et al.* 2014; Pierik 2017). In the Rhine-Meuse delta flooding frequency and intensity increased between 1700 cal. yr. BP and 1100 cal. yr. BP and multiple avulsions are placed within this time frame (Stouthamer and Berendsen 2000; Erkens 2009; Toonen 2013; Cohen *et al.* 2016; Pierik *et al.* 2017). In the Dutch coastal area increased storm surges are observed from 1350 cal. yr. BP onward (Knol 1993; Vos and Van Heeringen 1997; Pierik *et al.* 2016). Contrastingly, a decrease in aeolian activity is visible during the Roman period (1950-1550 cal. yr. BP) in the Pleistocene cover-sand areas and an increase in driftsand activity took place at the end of the first millennium around 1050 cal. yr. BP (Pierik *et al.* 2018). Vegetation development during the first millennium AD is characterised by a reforestation phase between 1850 cal. yr. BP and 1250 cal. yr. BP. Although timing and magnitude vary, this reforestation trend is recognised at most palynological study sites in the Netherlands and neighbouring Germany (e.g. Teunissen 1990; Bunnik 1999; Kalis *et al.* 2008; Litt *et al.* 2009; Dörfler *et al.* 2012).

Although all climate, landscape, vegetation and population changes during the first millennium AD are concurrent and some relation among them seems indisputable, the exact influence of each of these factors remains unknown. It is therefore essential to obtain detailed and well-dated evidence of these changes to disentangle the cause and effect of human impact, climate, landscape and vegetation change during the first millennium AD.

Yet, detailed climate data from the Netherlands for the first millennium AD are at present not available. This is probably due to the scarcity of archives suitable to study for this important time interval. Pristine natural archives such as peat bogs and lake fills are often no longer present due to peat excavation, artificial drainage and other human disturbances. Lake Uddelermeer, located in a cover-sand area in the central part of the Netherlands, is a unique site as it contains an undisturbed sediment profile covering the last ca. 14,000 years (Engels *et al.* 2016).

Chironomids, or non-biting midges, are an excellent proxy for the reconstruction of past summer temperatures because they have a short life cycle and are sensitive to changes in temperature (Brooks *et al.* 2007; Telford and Birks 2011; van Asch 2012; Heiri *et al.* 2014). They have mainly been used to study Lateglacial temperature variability but have been proven to be good proxy for Holocene temperatures as well (Axford *et al.* 2009; Millet *et al.* 2009; Brooks *et al.* 2012; Nazarova *et al.* 2013). However, as a result of human interference in the environment, chironomid-inferred temperature reconstructions for the Late Holocene can be problematic. Even small-scale human impact such as Prehistoric farming has been shown to impact chironomid communities and distort the climate signal (Taylor *et al.* 2013; Taylor *et al.* 2017a; Taylor *et al.* 2017b). Therefore, a multi proxy approach is recommended as a method for Holocene climate reconstructions, to infer possible human impact on

the record, and to disentangle the effects of natural processes such as climate change from anthropogenic impacts on the landscape (McKeown and Potito 2016; Taylor *et al.* 2018).

The aims of this study are fourfold: (1) to present the first chironomid record from the Netherlands covering the first millennium AD on a multi-decadal scale, (2) to determine, using the sedimentological, palynological and chironomid records, to what extent human impact influenced the lake ecology and whether temperature is the main environmental driver of changes in the chironomid assemblage, (3) to assess whether absolute chironomid-inferred summer-temperature values are realistic and, (4) to assess whether the chironomid-inferred temperature reconstruction shows evidence for temperature change during known phases of changing climate.

2 Area description

Lake Uddelermeer is a pingo remnant located on the Veluwe (52º14'48''N; 5º45'40''E; 24-27 m a.s.l.) (Fig. 1). The pingo remnant is situated at the head of a periglacial valley, in the cover-sand area between the ice pushed ridges of Ermelo (max. elevation ca. 50 m a.s.l.) and Apeldoorn (max. elevation ca. 100 m a.s.l.) (Fig. 1) and in the subsurface an impermeable clay layer is present. These boundary conditions are typical for the occurrence of pingos in the Netherlands due to the presence of a ground water gradient and/or pressure. This is evidenced by the presence of another pingo remnant in this area: Lake Bleekemeer, which does not contain a complete Late Holocene lake infill due to peat cutting (Polak 1959).

Lake Uddelermeer is oval shaped, 200-300 metres in diameter and has a current maximum water depth of 1.3 metres (Engels *et al.* 2016). The total lake sediment infill reaches a maximum depth of 15.6 metres of which 12.9 metres covers the Holocene. The lake is fed by groundwater and a small brook is draining the south-side of the lake (Staverdense or Leuvenumse beek). The area directly surrounding the lake is slightly elevated, limiting inflow of surface water runoff into the lake (Fig. 1). The lake is currently eutrophic and directly surrounding the lake is an alder carr and a fringe of wetlands with reeds. The regional vegetation consists mainly of mixed oak and birch forest, grasslands and agricultural fields. Average July temperature for the period 1901-2017 in de Bilt (ca. 50 km SW of Lake Uddelermeer) is 16.95 °C (1901-1950 = 16.4 °C) (Royal Netherlands Meteorological Institute; www.knmi.nl)

Archaeological finds in the vicinity of the lake indicate the presence of human activities from the Middle Mesolithic onward (Groenewoudt *et al.* 2006). Neolithic (7250-3950 cal. yr. BP; 5300-2000 BC) burial mounds from the Trechterbeker culture (5350-4850 cal. yr. BP; 3400-2900 BC) are present at a distance of ca. 500 metres from the lake. There is also evidence of charcoal production in the direct surroundings of the lake during the 9th and 10th centuries (Kraanen and Pape 1965). Situated next to the lake is a medieval structure dating to the late 10th century (Heidinga 1987). This so-called Huneschans is a medieval ring fort (*ringwalburg*) which is approximately 100 metres in diameter, and is surrounded by a circular earthen wall and an outer ditch. The earthen wall is not fully circular, with an opening present on the side of the lake. The wall currently does not reach the lake itself, indicating that the water level of the lake was up to 1.7 metres higher during the time of construction of the fort (10th century; Engels *et al.* 2016). Earlier palynological studies by Engels *et al.* (2016), Bohncke (1999), Sohl (1983) and Polak (1959) show the first evidence of human activities at the beginning of the Subboreal at 5000 cal. yr. BP, which is concurrent with the construction of the burial mounds encountered in the area (Groenewoudt *et al.* 2006). Pollen records covering this period show an increase of *Corylus* and *Pteridium* indicating open forests as well as the occurrence of human indicators such as *Plantago* and Cerealia. From 4000 cal. yr. BP onward the human-induced deforestation trend, which initiated around 5000 cal. yr. BP, increased.

Human presence in the form of agriculture is continuous from 3450 cal. yr. BP onwards as indicated by a continuous Cerealia pollen curve (Engels *et al.* 2016).

Figure 1 around here

3 Methods

A 16-metre-long sediment core (ø 6 cm) was collected from the deepest part of the lake in April-May 2012 using a piston corer operated from an UWITEC coring platform. The lake infill was cored in 3 metre sections using overlapping cores, and coring tubes were subsequently cut to 1 metre intervals in the field to enable transport. In the lab the core segments were cut in half lengthwise, where one part was completely preserved and the other half was used for sampling. A continuous 1 cm sampling was carried out for Loss on Ignition (LOI) to determine organic content following the protocol by Heiri *et al.* (2001). A total of 437 samples of ca. 1 cm^3 were dried at 105º C for 12 hours and subsequently placed in an oven at 550º for 4 hours. The samples were weighed before and after each step, obtaining both the moisture as well as the organic carbon content. Pollen samples of 0.7 cm^3 were collected using a 5 cm sampling resolution for the section 100-500 cm below the sediment/water interface to obtain a high-resolution vegetation record capable of detecting the fast vegetation changes during the first millennium AD in detail. In total 70 pollen samples were prepared following the method described in Faegri and Iversen (1989) and Moore *et al.* (1991). Identification of pollen, spores and Non Pollen Palynomorphs (NPPs) was executed using a Zeiss microscope with 400x magnification and pollen and spores were identified using Beug (2004), Moore *et al.* (1991) and Punt (1976; 1980; 1981; 1984; 1988; 1991; 1995; 2003). NPPs such as algal remains and (fungal) spores were identified using van Geel *et al.* (2003), van Geel (1978) and van Geel (1972). An upland pollen sum of 300 pollen grains, excluding alder and grasses, was counted per sample. This pollen sum differs from the one used in Engels *et al.* (2016), as grasses and alder pollen are excluded from the pollen sum in this study since reed land (included in the Poaceae curve) and alder carr occur locally.

The sediment record was previously analysed for chironomids at a coarse temporal resolution by Engels *et al.* (2016). For the current research, additional chironomid samples were analysed to increase the temporal resolution from the section 200-500 cm below the sediment surface to detect the short climatic phases during the first millennium AD. From this section, a total of 31 samples were analysed at 5-25 cm resolution. In order to get a better overview of preceding and subsequent trends, the lower temporal resolution results from Engels *et al.* (2016) from the sections 100-200 cm and 500-550 cm are also included in this study. Sample preparation for these samples is described in Engels *et al.* (2016). The additional samples (14 in total, sample size: 0.335 cm^3) were added to a 5% KOH solution, heated to 90°C for 1 hour, and then passed successively through 212 µm and 90 µm mesh sieves. Chironomid head capsules were manually picked out of the sieving residues using a Bogorov sorting tray under a dissection microscope (40x magnification) and subsequently mounted on permanent slides in Euparal©. Chironomid head capsules were identified under a compound microscope (magnification 400x) following keys by Wiederholm (1983), Moller Pillot (1984a); Moller Pillot (1984b), Rieradevall and Brooks (2001) and Brooks *et al.* (2007). Information on chironomid ecology was derived from a.o: Moller Pillot and Buskens (1990), Brooks *et al.* (2007), Moller Pillot and Klink (2009), Engels and Cwynar (2011), Luoto (2011), Engels *et al.* (2012), Moller Pillot (2013) and Potito *et al.* (2014). The number of identified chironomid head capsules varied between 65 and 146 per sample. A Principal Component Analysis (PCA) with Square-root-transformed percentage-abundance data of the chironomid taxa was executed using the program C2 (Juggins, 2003).

The chironomid assemblages were subsequently used to quantitatively reconstruct mean July air temperatures. This reconstruction was executed using a chironomid-temperature inference model, which is based on a modern calibration dataset that consists of 274 lakes from Norway and the Alpine regions (Heiri *et al.* 2011).

This chironomid-climate calibration dataset spans a July air temperature range from 3.5 to 18.4°C (Heiri *et al.* 2011). For the model, a two component weighted averaging partial least-squares (WA-PLS) regression was used since this approach produced inference models with the lowest error (Heiri *et al.* 2011). The selected model had a bootstrapped root mean square error of prediction of 1.40°C after outlier deletion (Heiri *et al.* 2011). Bootstrapping was used to estimate the sample-specific errors for the fossil samples.

We evaluated the robustness of the chironomid-inferred July air temperature reconstruction by calculating the closest modern analogue of the fossil samples, as well as the goodness-of-fit to temperature (Birks *et al.* 1990) and the cumulative percentage of rare or absent species from the calibration dataset. The closest modern analogue was assessed based on squared Chi-squared distances using the program C2 (Juggins, 2003). Fossil samples with a distance to the closest analogue larger than the 2nd and 5th percentile of the distances of the modern samples in the calibration dataset were classified as having 'no close' and 'no good' analogue, respectively. Goodness-of-fit to temperature was assessed using a Canonical Correspondence Analysis (CCA) of the modern samples with temperature as the only constraining variable. In this analysis, the fossil samples were added passively. Fossil samples with a residual distance exceeding the 90th and 95th percentiles of the residual distances of the modern samples were identified as having a 'poor' and 'very' poor fit with temperature, respectively. The CCA was calculated using CANOCO for Windows version 4.51 (ter Braak and Šmilauer 2012). Both the pollen percentage diagram as well as the chironomid abundance diagram where produced using TILIA (Grimm 1991-2015). Zonation of the pollen and chironomid diagrams differs from Engels *et al.* (2016) as a result of the increased sampling resolution in this study and was established visually. The pollen diagram was subdivided into zones based on variations in the main pollen taxa and zonal boundaries were verified using CONISS (Grimm 1991-2015). The chronology of the core is based on the age-depth model of Engels *et al.* (2016), which is based on 26 samples for ^{210}Pb measurement for the top 65 cm of the core and 13 AMS radiocarbon samples (excluding 3 outliers) throughout the rest of the core. The age-depth model was produced using Bayesian modelling as included in Oxcal (Bronk Ramsey 2009). The radiocarbon samples contained terrestrial macrofossils, wood fragments and charred material such as grass epidermis and charcoal (Engels *et al.* 2016). The age-depth chronology of the core section discussed in this paper (100 to 550 cm sediment depth) is supported by six radiocarbon dates (excluding 1 outlier) and constrained at the top by the ^{210}Pb dates (Fig. 2). The resultant age-depth model gives well-constrained age estimates and a nearly linear sedimentation rate, confirming the reliability of the six dates included. All ages provided in this paper are rounded to the nearest five year interval and are expressed in cal. yr. BP unless explicitly stated otherwise.

Figure 2 around here

4 Results and interpretation

4.1 Sedimentology

The investigated core interval consists entirely of gyttja (Fig. 3). The bottom part, 550 cm up to 220 cm depth, consists of brown gyttja. From 220 cm upward this slowly shifts to a more greenish gyttja, indicating a larger component of algae. The LOI-record follows this trend with values around 60% from 550 cm up to 460 cm depth, followed by a more organic-rich sequence with values upward of 70%, until 270 cm depth. From 270 cm to 220 cm LOI values vary around 60% again and drop sharply to only 20% at 220 cm, which corresponds with the shift to a higher algal content. The drop in organic content is probably the result of increased silica production (a.o. diatom production) in the lake. Alternatively, an increase in sand input through increased aeolian activity could explain this decrease. However, no visible sand grains were found during visual core inspection, suggesting

that an increase of silica production is the most likely reason for the observed decrease in LOI values. From 220 cm upwards, LOI values gradually increase, reaching 60% at 140 cm after which they gradually decrease to 30%.

Figure 3 around here

4.2 Palynology

Zone Pa (500-382 cm depth; 2420-1730 cal. yr. BP) is characterised by high values of Arboreal Pollen (AP) and heather (Fig. 3). High values of deciduous tree species such as *Quercus, Fagus* and the occurrence of *Carpinus*, *Tilia* and *Ulmus* suggest the presence of a mixed-deciduous forest in the vicinity of the lake. *Fraxinus*, *Corylus* and *Betula* probably grew at the forest edge or in small bushes and thickets. Human presence in the area around Lake Uddelermeer is indicated by high percentages of upland herbs with typical anthropogenic indicators such as *Rumex*, *Plantago lanceolata* and *Artemisia vulgaris* and the presence of pollen grains of Cerealia, indicating arable fields nearby. Heathlands are also present in the area, as evidenced from the large proportion of *Calluna*. The lake was probably surrounded by an alder carr with grasslands in the vicinity and alder carr was likely also present in the brook valley of the Leuvenumse beek to the south. The high values of both *Isoëtes* and *Littorella* suggest relatively nutrient-poor and clear-water conditions in the lake itself. *Isoëtes* and *Littorella* are both adapted to low nutrient conditions, by a symbiosis with mycorrhiza to enable carbon uptake from the sediment, and a slow growth rate, and are therefore typical inhabitants of oligotrophic lakes, where they most often grow in water of 0 to 2 metres deep (Sand-Jensen 1978; Weeda *et al.* 1988; Engels *et al.* 2018). *Isoëtes* can grow in water up to 4.5 metres deep and prefers a sandy subsoil (Sand-Jensen 1978; Farmer and Spence 1986). Most likely *Littorella* also grew at the shore of the lake, since this species only flowers when it is not submerged (Weeda *et al.* 1988). Together, both species form the *Littorellion* which is a relatively stress tolerant plant community (Rørslett and Brettum 1989). However, when nutrient availability increases, macrophytes and algae can more easily inhabit the lake. As a result *Littorella* and *Isoëtes* receive less light and the *Littorellion* is fast replaced by reedlands (Weeda *et al.* 2000). The nutrient-poor conditions in the lake are confirmed by the presence of *Nymphaea alba* which probably grew in the deeper parts of the lake. The algae *Botryococcus,* which was present in Lake Uddelermeer continuously since the Late Glacial (Engels et al., 2016), can occur in a wide range of environments but has a preference for oligotrophic lakes (Padisák *et al.* 1998). Engels *et al.* (2016) reconstructed a water depth of around 2.5-3 metres during this time period, which is in line with the 2 metres suggested by the aquatic taxa present in the lake. Spores of *Glomus,* a fungus often found in soils, is present in the upper part of this zone. The occurrence of *Glomus* spores in lake sediments is indicative of soil erosion (van Geel *et al.* 2003).

Zone Pb (382-255 cm depth; 1730-1270 cal. yr. BP) is characterised by increasing values of AP and decreasing values of heather and to a lesser extent upland herbs (Fig. 3). The increase in AP can be mainly attributed to *Quercus, Fagus* and *Carpinus*. Anthropogenic indicators such as upland herbs (*Rumex, Plantago lanceolata* and *Artemisia vulgaris)* and Cerealia decrease in this zone. Pollen grains of Cerealia are still present, albeit in low abundances, and occasionally *Secale cereale* is found. These changes in the pollen assemblage suggest that deciduous forests have expanded at the expense of heathlands and arable lands. We also observe an increase of *Alnus* and a decrease of Poaceae suggesting that the local alder carrs are also expanding. The basal cells of Nymphaeaceae (NPP type HdV-127) are decreasing sharply during this zone, although *Nymphaea alba* is still present in the pollen record. *Nuphar lutea,* however, is nearly absent from zone Pb. The continued presence of *Isoëtes* and *Littorella* suggests continued nutrient-poor and clear-water conditions in the lake. Pollen-percentage values of *Littorella* however, are slightly decreasing. The occurrence of *Typha latifolia* pollen during this zone indicates the presence of reed lands at the lake fringe which possibly partly replaced the *Littorellion*.

Zone Pc (255-220 cm depth; 1270-1140 cal. yr. BP) is a transitional zone which shows decreasing AP values and increasing values of Cerealia and heather (Fig. 3). A mixed deciduous forest is still present but arable lands and heathlands are fast expanding. This is also visible from the increase in anthropogenic indicators such as Cerealia*, Plantago lanceolata,* a continuous curve of *Secale cereale* pollen, and an increase in the occurrences of charcoal. The alder carr decreases in size and becomes more open with more grass or reed land, as seen from the decreasing abundance of *Alnus* and increasing Poaceae values and the presence of *Typha angustifolia. Isoëtes* and *Littorella* are still present in the pollen record indicating relatively stable conditions in the lake through zone Pa, Pb and Pc. The water body must have remained clear enough throughout pollen zones Pa, Pb and Pc to sustain the *Littorellion*.

Zone Pd (220-100 cm depth; 1140-320 cal. yr. BP) is characterised by further decreasing values of AP and heather and increasing values of upland herbs and Cerealia (Fig. 3). The start of this zone is simultaneous with the shift to green algal gyttja indicating a higher production in the lake. This is also evident from the rapidly increasing values of algal remains such as *Scenedesmus* or *Pediastrum*. An increase in various algal species from ca. 25% to over 100% occurs at 185 cm depth (1030 cal. yr. BP). In our record the abrupt increase in algal remains coincides with increasing values of fungal spores of coprophilous fungi such as *Sporormiella, Podospora* and *Cercophora* which are indicative for the presence of dung. The increase in algae also coincides with the habitation phase of the Huneschans (late 10th cent.) and is most likely caused by increased nutrient input as a result of human impact. Engels *et al.* (2018) however, found sediment age and water depth to be the most likely explanatory variables for this ecosystem change. From 155 cm depth (1250-700 cal. yr. BP) onward *Cannabis*-type shows an increase from ca. 1% to ca. 35% which is likely the result of the retting of hemp in the lake to create hemp fibres for rope production. The practice of hemp retting in the Netherlands is known from the historic record and also evidenced at Lake Uddelermeer from the high values of *Chaetomium* spores which are cellulose-decomposers and occur among others, on decaying herbaceous stems (van Geel *et al.* 2003).
Overall zone Pd indicates an increase in human activity, with higher values of Cerealia, *Secale, Fagopyrum* and *Sinapis*-type and various herbs such as *Rumex* and Amaranthaceae. The presence of charcoal also increases during this zone, which might be linked to the charcoal production in the area. There are fewer deciduous tree species present indicating the disappearance of the closed and mixed deciduous forest, which are being replaced by more open oak forest with hazel and ash. Arable lands are expanding while the heathlands are decreasing. The alder carr is also disappearing and is being replaced by grassland. In the lake itself the eutrophic conditions are evident from the disappearance of *Littorella, Isoëtes* and *Nymphaea* and the concurrent increase of *Myriophyllum alterniflorum*. The occurrence of this aquatic perennial is often linked to an increase in phosphate (Roelofs *et al.* 1984). *Myriophyllum alterniflorum* grows in water up to 2 metres deep (Hannon and Gaillard 1997) suggesting that water depth remained stable during the entire period, in line with results by Engels *et al.* (2016).

Figure 4 around here

4.3 Chironomid record

Chironomids are well preserved and abundant throughout the record. Our record has an average count sum of 99 head capsules per sample (range 64-167). Most of the encountered chironomid taxa (e.g. *Lauterborniella, Parakiefferialla bathophila*-type) are commonly found in the littoral zone of meso- to eutrophic lakes and prefer warm or temperate conditions (Brooks *et al.* 2007, and references therein). Further, a number of taxa present in the record are often associated with macrophytes (e.g. *Ablabesmyia*). The chironomid diagram is divided into two zones Ch1 and Ch2, following major shifts in the chironomid assemblage, which correspond with the major lithological units in the core (Fig. 4).

Chironomid zone Ch1 (550-220 cm; 2525-1140 cal. yr. BP) is dominated by *Lauterborniella*, *Cladotanytarsus mancus*-type and *Parakiefferiella bathophila*-type which are all typical inhabitants of littoral zones of lakes. In addition, *Lauterborniella* and *P. bathophila*-type are often associated with submerged vegetation (Moller Pillot 1984b; Brooks *et al.* 2007; Moller Pillot and Klink 2009; Moller Pillot 2013). *Lauterborniella* is found in the warmer lakes included in the Norwegian-Swiss calibration dataset (Heiri *et al.* 2011). Chironomid zone Ch1 is further subdivided based on smaller changes in the abundance of the chironomid taxa.

Subzone Ch1a (550-470 cm depth; 2525-2240 cal. yr. BP) is marked by relatively high values of *Endochironomus albipennis*-type and *Pseudochironomus* and the presence of *Limnophyes/Paralimnophyes* and *Procladius*. Both *Pseudochironomus* and *E. albipennis*-type occur in the littoral of lakes (Brooks *et al.* 2007; Engels *et al.* 2012). *E. albipennis*-type is often associated with macrophytes (Moller Pillot 1984b) suggesting the presence of aquatic vegetation in the lake. This is in line with the pollen record, which indicates the presence of a *Littorellion* and Nymphaeaceae. Based on the presence or *Littorella* and *Isoëtes,* relatively nutrient-poor conditions are expected in the lake. However chironomid taxa such as *P. bathophila*-type and *Polypedilum nubeculosum*-type are typically found in eutrophic lakes (Moller Pillot 2013). *Lauterborniella* is often ascribed to eutrophic conditions (Moller Pillot 2013) but this genus has been found in oligotrophic lakes as well (Brodin 1986). Based on the combination of the presence of aquatic macrophytes that typically occur in oligo- to mesotrophic conditions and chironomid taxa that typically occur in meso- to eutrophic conditions we conclude that the lake was probably mesotrophic throughout zone Ch1. This conclusion is further supported by the occurrence of taxa such as *Pseudochironomus and Tanytarsus mendax*-type, which are inhabitants of mostly mesotrophic lakes (Moller Pillot 2013). Further, *Limnophyes/Paralimnophyes, Lauterborniella, P. nubeculosum* and *Pseudochironomus* are most often found in shallow lakes (Brooks *et al.* 2007; Engels *et al.* 2012), which is in line with the presence of the *Littorellion* and the estimated water depth of 2.5 to 3 metres by Engels et al (2016). *C. mancus*-type and *P. bathophila*-type have a preference of lakes with a water depth less than 5 metres (Luoto 2011). The majority of species present in this zone such as *E. albipennis*, *Procladius*, *C. mancus*-type are acidophilic which is also in line with the reconstructed nutrient-poor, clear-water conditions in the lake. In the calibration dataset, *Procladius* and *Limnophyes/Paralimnophyes* are both found along a large temperature gradient, including colder lakes, resulting in relatively low temperature optima for these taxa (Heiri *et al.* 2011).

The onset of subzone CH1b (470-390 cm depth; 2240-1760 cal. yr. BP) is defined by the appearance of *Parachironomus varus*-type and an increase of *Corynoneura edwardsi*-type and further characterized by the absence of *Limnophyes/Paralimnophyes* and *Procladius. P. varus*-type *and C. edwardsi*-type are both often associated with macrophytes and have relatively high temperature optima in the Norwegian-Alpine calibration dataset (Heiri *et al.* 2011) (Brooks *et al.* 2007). At the start of this subzone, *E. albipennis*-type reaches maximum values, directly followed by a strong decline from 19.2 % to 1.4%. *Lauterborniella* also reaches maximum values in this subzone. *Pseudochironomus* is still present, although at slightly lower abundances than in the previous subzone. *P. varus*-type is acidophobic (Brooks *et al.* 2007) suggesting less acidic conditions which is in line with the drop in *Procladius* and *E. albipennis*-type which are both acidophilic. Nevertheless, other acidophilic species such as *C. mancus*-type, *Psectrocladius sordidellus*-type are still present. We therefore conclude that the shift in the chironomid fauna associated with the Ch1a/Ch1b-transition does not reflect any significant changes in the lake ecosystem but rather a reorganization of the fauna already present in the lake.

Subzone Ch1c (390-255 cm depth; 1760-1270 cal. yr. BP) is defined by maximum values of *P. bathophila*-type (35.7%) and is further marked by the reappearance of *Limnophyes/Paralimnophyes* and *Procladius* and an increase in *P. sordidellus*-type and *P. nubeculosum*-type. *Lauterborniella* gradually declines from its maximum abundance of 35.2% to values of 15.3% during subzone Ch1c. *Pseudochironomus* and *P. varus*-type also reach lower abundances than in the previous subzone. Both *P. nubeculosum*-type and *P. sordidellus*-type typically occur in the littoral zone of temperate lakes (Engels *et al.* 2012; Luoto 2012), although

according to Moller Pillot (1984b) *P. nubeculosum*-type is found in lakes with a depth up to 18 m. The increase in *P. nubeculosum*-type, *P. bathophila*-type might suggest more nutrient-rich conditions in the lake. However, oligotrophic and mesotrophic taxa such as *Heterotanytarsus* and *Pseudochironomus* are still present indicating that conditions remained relatively nutrient poor.

The final subzone (Ch1d: 255-220 cm depth; 1270-1140 cal. yr. BP) is marked by higher values of *E. albipennis*-type, while abundances of *Lauterborniella* and *P. bathophila*-type are lower than in the preceding subzones. Taxa that appear or increase during this zone are *Glyptotendipes pallens*-type and *Polypedilum sordens*-type which are both found in the warmer lakes in the training set. The most distinct feature of this subzone, however, is the high abundance of *T. mendax*-type. This taxon consists of a large number of species and is found in a range of environments (Brooks *et al.* 2007). The taxon also occurs along a wide temperature range, but is absent from the coldest lakes (Heiri *et al.* 2011). *T. mendax*-type is sensitive to increases in phosphate but can occur in all trophic states and prefers mesotrophic conditions. This species mostly lives in the profundal zone and is most abundant in water over 5 metres deep. *E. albipennis*-type and *P. bathophila*-type have similar nutrient preferences although *P. bathophila*-type is indicative for warmer conditions. The shifts that we observe in the chironomid fauna during zone Ch1 do not coincide with shifts in ecology of the lake as reconstructed from the pollen and LOI records. We therefore suggest that the changes observed in the chironomid record were potentially driven by external factors such as climate change rather than by changes in within-lake processes.

The onset of chironomid zone Ch2 coincides with the transition of brown gyttja to green algal gyttja (220-100 cm depth; 1140-320 cal. yr. BP). Zone Ch2 is marked by increases or appearances of the chironomid taxa *Microtendipes pedellus*-type, *Cladopelma lateralis*-type, *Cricotopus laricomalis*-type, *Nanocladius branchicolis*-type and the Tanypodinae *Procladius* and *Ablabesmyia.* Zone Ch2 also shows an increase in the total number of chironomid taxa found, with a maximum of 25 taxa at 149 cm. Of the dominant taxa in zone Ch1, *C. mancus*-type and *P. bathophila*-type are still present in zone Ch2, while *Lauterborniella* strongly declines towards the upper part of this zone. In addition, the chironomid assemblage still includes a.o. *E. albipennis*-type, *P. nubeculosum*-type and *T. mendax*-type. Both the sedimentological and the palynological record indicate a strong shift in the water quality of the lake during this time period, with more nutrient-rich and turbid conditions present after 1140 cal. yr. BP. This transition is reflected in the chironomid-species composition where most species with specific habitat requirements such as the presence of aquatic macrophytes or low-nutrient levels decline in favour of *Procladius* and *Ablabesmyia.* These latter two taxa are typically interpreted as generalists and are able to persist in dynamic conditions (e.g. Vallenduuk and Moller Pillot 2007). *Ablabesmyia* prefers shallow, warm and still water and is associated with macrophytes (Engels *et al.* 2012). Additionally, *Procladius* is sensitive to increases in phosphate, can occur in acidified lakes and tolerates pollution well (Luoto 2011). *M. pedellus*-type is also often encountered in dynamic environments and together with *Ablabesmyia* is found in shallow lakes of less than five metres deep (Engels *et al.* 2008a; Engels *et al.* 2008b; Engels *et al.* 2012). Potito *et al.* (2014) found a relation with high agricultural cover and the occurrence of this chironomid taxon, which is in line with the low AP values and high upland herbs and Cerealia pollen percentages in this zone. *M. pedellus*-type however, has a preference for mesotrophic conditions and a stable oxygen regime (Moller Pillot and Klink 2009), and Engels *et al.* (2018) therefore suggested that this increase could be a relative increase, with other taxa decreasing faster under unfavourable conditions than *M. pedellus*-type. Other taxa that indicate higher trophic conditions are e.g. *G. pallens*-type, *Chironomus anthracinus*-type, *Chironomus plumosus*-type, *C. lateralis*-type, *Dicrotendipes nervosus*-type. Overall, the combined proxy-records indicate a shift in the lake ecology from the clear-water mesotrophic conditions of zone Ch1 to the eutrophic, turbid conditions of zone Ch2.

Figure 5 around here

4.4 Factors controlling the chironomid fauna composition of Lake Uddelermeer

The most important precondition to establish a C-IT reconstruction is that temperature fluctuations are the main factor influencing the chironomid composition. This is especially important for Holocene temperature reconstructions, since the amplitude of temperature fluctuations in e.g. the mid-latitudinal areas of the northern Hemisphere, was small when compared to Late Glacial studies. Chironomid communities of shallow, temperate lakes such as Lake Uddelermeer are especially sensitive to changes in the environment since dominant controls on the chironomid composition like hypolimnetic oxygen depletion and climatic extremes are lacking (Langdon *et al.* 2006). Based on the sedimentological, palynological and chironomid record, conditions in the lake itself remained stable with clear-water, nutrient-poor conditions during the interval between 2500 and 1140 cal. yr. BP i.e. covering chironomid zone Ch1 and the pollen zones Pa, Pb and Pc. The strong eutrophication of the lake at the onset of chironomid zone Ch2 is visible in the sediment core as a colour change, in the pollen record (here zone Pd) as an increase in algal species, and in the chironomid record as an increase of generalists such as *Ablabesmyia* and *Procladius* (Fig. 5). Together these changes indicate a significant ecosystem shift in Lake Uddelermeer from mesotrophic clear-water conditions to more nutrient-rich and turbid conditions. This conclusion is in line with results by Engels et al. (2018), who reconstructed stable clear-water conditions in Lake Uddelermeer from 6000 cal. yr. BP onward and an increase in nutrient availability at 1030 cal. yr. BP from sedimentary pigments, chironomids and pollen. Engels *et al.* (2018) placed the change to turbid lake-water conditions at 1030 cal. yr. BP, which corresponds to the maximum increase in algae abundances at 185 cm in the pollen data. Our high-resolution record indicates that the first onset of change occurred from 1140 cal. yr. BP onward, with increasing percentages of algae and fungal spores and decreasing pollen percentages of *Littorella* and *Isoëtes* and a shift to brown-green gyttja (Fig.5).

The pollen record additionally indicates changes in the regional vegetation during the investigated period, with a reforestation phase in zone Pb from 1730 till 1270 cal. yr. BP (Fig. 5). These regional changes in forest cover did not result in significant changes in the aquatic vegetation in the lake during Ch1. It is possible that the presence of a slightly raised area surrounding Lake Uddelermeer, as seen on the LIDAR elevation map (Fig. 1), limited inflow of surface water runoff into the lake from the surrounding area, limiting the impact of regional changes in land use. Increased sediment and nutrient input into the lake as a result of agriculture and deforestation are often the main actor in ecosystem changes in lakes. Potito *et al.* (2014) identified agricultural land cover as one of the most dominant environmental variables influencing chironomid composition. Nevertheless, chironomid inferred temperatures can still be valid from these lakes when agriculture remained stable during the investigated time period (Potito *et al.* 2014). From the pollen record the presence of agriculture in the area was evident, albeit in low percentages which remained constant in pollen zones Pa and Pb and only slightly increased during Pc. In addition, consistently high lake levels are reconstructed for the investigated period (Engels *et al.* 2016), suggesting that changes in water level, which could also affect the chironomid assemblages (Engels and Cwynar 2011), did not play a role either. We therefore conclude that environmental conditions in the lake remained stable in the period between 2525 cal. yr. BP and 1140 cal. yr. BP and suggest that the chironomid record could provide a reliable temperature reconstruction for this period. The chironomid fauna that was existent during the formation of the upper samples (220-100 cm depth), obtained from the green algal gyttja (Ch2), was strongly influenced by the local eutrophication process. These samples are therefore deemed unreliable for temperature reconstruction purposes and will not be discussed.

Figure 6 around here

4.5 Chironomid-inferred mean July air temperature reconstruction

Reconstructed mean July air temperature values vary between 16.1 and 19.1°C with an average reconstructed temperature of 17.6°C (Fig. 6). This places the reconstruction in the upper part of the temperature range of the calibration dataset (3.5-18.4 °C) (Heiri *et al.* 2011). Sample-specific errors range between 1.4 and 1.6 °C.

A number of temperature fluctuations can be observed between 2525 and 1140 cal. yr. BP. At the start of the investigated period (2525-2240 cal. yr. BP, or 550-470 cm depth), mean July air temperature values are low, with an average temperature of 17.4°C. For the period between 2240 and 1760 cal. yr. BP (470-390 cm), slightly higher temperatures are reconstructed, with an average temperature of 18.6°C. Maximum reconstructed temperatures of 19.1°C are reached at a depth of 464 cm (2197 cal. yr. BP). Slightly colder conditions, with an average mean July air temperature of 17.1°C, prevailed in the period between 1760 and 1280 cal. yr. BP (390-255 cm). The coldest phase is reconstructed from 330-304 cm (1551-1465 cal. yr. BP) with an average mean July air temperature of only 16.5°C. This is followed by slightly higher (average 18.3°C) values for the period between 1280 and 1140 cal. yr. BP (255-220 cm).

The down-core evaluation analyses suggest that most chironomid assemblages in the fossil record are classified as having both ‘no close’ or ‘no good’ modern analogue and a ‘poor’ or ‘very poor’ fit with temperature. Only two samples contain taxa which are not included in the calibration dataset, reaching values of maximum 2%. Therefore, even though the composition of the chironomid assemblages in the fossil record differs from the modern assemblages, the individual taxa in the fossil samples are well represented in the modern samples. WA-PLS can perform relatively well in no-analogue conditions as long as the majority of the chironomid assemblage is well represented in the calibration data set (Birks 1998).

Reconstructed mean July air temperatures in part, exceed the maximum mean July air temperature of the modern samples in the calibration dataset of 18.4 °C. This might have affected the absolute values of the temperature reconstruction. The magnitude of the observed fluctuations (1.39-1.56 °C) is similar to the sample-specific error of the reconstructed temperatures. Nevertheless, the fluctuations are recorded in multiple samples on a high temporal resolution, thus giving a consistent picture of these temperature changes. Moreover, observed fluctuations approximately coincide with shifts in the chironomid assemblage. For example, during the two colder oscillations, taxa with relatively low optimum temperatures are present, such as *Limnophyes/Paralimnophyes*, *Procladius* and *P. sordidellus*. Similarly, the sample with the highest reconstructed mean July air temperature (464 cm) coincides with maximum abundances of *E. albipennis*-type, which is found in the warmer lakes of the calibration dataset (Heiri *et al.* 2011) suggesting that temperature is indeed the main driver of the chironomid fauna in this part of the record. When we compare the reconstructed C-IT from Lake Uddelermeer to the average July temperature of 17 °at de Bilt (50 km SW of Lake Uddelermeer) for the period 1901-2017 it seems that our reconstructed temperatures are relatively high. Even during the DACP reconstructed temperatures are similar to recent conditions (17 °C vs. 17.1°C) indicating that the record is likely overestimating the absolute temperature. Potito *et al.* (2014) found that sites with agriculture in their catchment can overestimate temperature as a result of increased production in the lake. Other chironomid records from NW Europe also indicate that temperature during the DACP was at least 1°C lower than current temperature values (Northern England: Langdon *et al.* 2004; Barber *et al.* 2013; Cairngorms UK: Dalton *et al.* 2005; northern Alps: Millet *et al.* 2009). Additionally, the reconstructed temperature range is located in the upper ranges of the Norwegian/Alpine training set which could result in so called edge-effects. It therefore seems likely that the absolute values of our C-IT reconstruction overestimate past July air temperatures.

5 Discussion

Based on the chronology of the record, we can correlate the observed temperature oscillations in the record to climate fluctuations as recorded in the Northern Hemisphere (e.g. Ljungqvist 2010). The slightly higher reconstructed temperatures in the period from 2240-1760 cal. yr. BP probably correspond with the RWP. The subsequent cold phase (1760-1280 cal. yr. BP) can be correlated to the DACP. The warmer conditions reconstructed for the upper part of the record (1280-1140 cal. yr. BP) can be linked to the MCA (Fig. 6). The C-IT record shows that temperature during the Iron Age (till 2240 cal. yr. BP) was lower than during the RWP by an estimated 1.2 °C. To evaluate the representability of these temperature trends in NW Europe we will first compare our results to other C-IT records. In a second step we will compare our results to other available climate reconstructions from NW Europe including detailed tree-ring records and global data compilations.

Figure 7 around here

5.1 Chironomid-inferred temperature reconstructions from NW Europe

To our knowledge only two other Late Holocene C-IT reconstructions, which have been identified as representative NW-European temperature trends for the period discussed here, are available. Both of these sites are located in Northern England: Talkin Tarn (Langdon *et al.* 2004) and Bigland Tarn (Barber *et al.* 2013). A RWP, a distinct DACP and the MCA can be distinguished in the record from Bigland Tarn (Fig. 7). These phases might also be visible in the record from Talkin Tarn, although the comparison with that record is less robust, due to the lower sampling resolution and uncertain chronology of that site. The similarity between the three sites, both in timing as well as amplitude of temperature change, suggests that the reconstructed temperature fluctuations in Lake Uddelermeer record reflect a regional climate signal. The overall trend of the reconstruction from Uddelermeer is very similar to that of Bigland Tarn and Talkin Tarn. The RWP is the warmest phase in the Uddelermeer record with an increase in temperature of 1.2 °C compared to the Iron Age. This is similar to the increase in the Bigland Tarn record of 1°C. The average temperature drop from the RWP to the DACP in the Uddelermeer record is 1.5 °C whereas this shift in the Bigland Tarn record is slightly bigger with 2.2 °C. The MCA forms the warmest period in the Bigland Tarn record with an average temperature of 13.7°C. The MCA in the Uddelermeer is only partly present and as seen in the Bigland Tarn record, the first part is not the warmest part of the period. When we compare absolute values of the independent reconstructions, it becomes apparent that reconstructed temperatures from both sites in England are consistently lower by 4-5 °C than the reconstruction from Lake Uddelermeer (Fig. 7). This could in part be the result of the more western location and higher elevation of these sites. The current average July temperatures of both Bigland Tarn as Talkin Tarn are around 15°C, compared to the average July temperature of 17°C at Uddelermeer. Additionally, previous studies have shown that the application of different chironomid-climate calibration datasets to the same fossil record will yield C-IT records that are up to several degrees different in absolute reconstructed temperatures (e.g. Engels *et al.* 2014; Bajolle *et al.* 2018). The temperature reconstructions from England are based on the Norwegian calibration dataset, which has a lower maximum temperature (16 °C; Brooks and Birks 2000) than the extended and combined Swiss-Norwegian dataset used for the reconstruction from Uddelermeer (18.4 °C; Heiri *et al.* 2011). However, it is likely that a large part of the difference in absolute temperatures is the result of a temperature overestimation in the record from Lake Uddelermeer.

Figure 8 around here

5.2 Regional evidence from the NH for the RMP, DACP and MCA

When we compare the start and end dates of the climatic phases indentified in the record from Uddelermeer to other temperature reconstructions and overviews from the Northern Hemisphere we observe that overall there is a good match between the available records (Fig. 8). All datasets shown in Fig. 8 show a similar starting date for the MCA, which is placed around 1300 cal. yr. BP. The start of the DACP shows slightly more variation in timing with starting dates ranging between 1536-1760 cal. yr. BP. Taking into account all age uncertainties it is likely that all records and overviews show the same simultaneous event. The start of the DACP in Uddelermeer is the earliest of the available estimates with a suggested starting date of 1760 cal. yr. BP. The 500-year duration of the DACP in the Uddelermeer record is 150 years longer than the duration of the DACP in the tree-ring record presented by Büntgen *et al.* (2011).

The latter part of the DACP in the tree-ring record of Büntgen *et al.* (2011) dated at 1414-1290 cal. yr. BP (536-660 AD) was later termed the Late Antique Little Ice Age or LALIA (Büntgen *et al.* 2016). This LALIA shows a strong temperature decline and is causally linked to a cluster of volcanic eruptions in 1414; 1410 and 1403 cal. yr. BP (536, 540 and 547 AD). Büntgen *et al.* (2017) promote the substitution of the DACP by the LALIA. However, the LALIA has not been identified in a large range of proxies and sites, and falls within the previously defined DACP. Additionally, since the timing and the causality differ, with a link to volcanism for the LALIA and an unknown cause for the DACP, the LALIA cannot be used as a substitution of the DACP. It therefore seems more appropriate to refer to this cold stage as a whole as the DACP (sensu Helama *et al.* 2017b; Helama *et al.* 2017a). The Uddelermeer record does suggest a colder second part of the DACP which starts at 1550 cal. yr. BP and lasts till 1450 cal. yr. BP. It is possible that this colder phase reflects the LALIA, although the chronology of the cold period observed in our Uddelermeer record does not match the timing and duration observed in the tree ring record (Büntgen *et al.* 2017). More detailed and well-dated studies covering this time period would contribute to a better understanding of this coldest phase of the DACP.

An earlier start and a longer duration of the DACP in the Netherlands, compared to the DACP recorded in the tree ring record, could be the result of different local climatic conditions. Nevertheless, a longer and earlier DACP is in line with both the Bigland Tarn record as well as the two overview studies by Ljunqvist (2009) and Helama (2017). Aside from the tree-ring data set, the Uddelermeer chironomid record is the most detailed temperature record reconstructing absolute temperature values during the Dark Ages Cold Period in for NW Europe.

The start of the RWP cannot be identified in all studies presented in Fig. 8. In the Bigland Tarn and Uddelermeer records the start of the RWP is placed at 2365 cal. yr. BP and 2240 cal. yr. BP, respectively. Taking into account the error margins of the chronology of both studies, this could be a simultaneous event. In the tree-ring data set no clear RWP is evident, but the start of a warmer phase does coincide with the start of the RWP at Uddelermeer. However, this warm period as identified in the tree ring record (Büntgen *et al.* 2016) is interrupted by a colder phase. The reconstructed temperatures in Uddelermeer and Bigland Tarn are both stable during the RWP and show no evidence of a brief colder period. The most probable explanation for this discrepancy are different climatic conditions in the Alps in contrast to the lower lying sites, as well as differences in sampling resolution and proxy sensitivity. In the chironomid record from the northern French Alps by Millet *et al.* (2009), which is not interpreted as a representative temperature reconstruction for the first millennium, also no clear RWP was visible. Different climatic conditions might also explain the differences in duration and the start of the DACP across the European continent. Overall, the start and end dates of the different climatic phases fall within the dating uncertainties and current results indicate that especially the MCA and DACP and to a lesser extent the RWP can be considered as simultaneous events across NW Europe.

6 Conclusions

We presented the first high-resolution chironomid record for the late Subatlantic in the Netherlands from Lake Uddelermeer. Our data shows that in the period 2500 to 1140 cal. yr. BP the lake was mesotrophic with clear-water conditions and sustained a *Littorellion.* From 1140 cal. yr. BP onward a shift in the water quality was reconstructed with high-nutrient turbid conditions and a dominance of algal species. The conditions in the lake in the period 2500-1140 cal. yr. BP do not signal large ecological changes or effects of human impact and thus suggest that this record is suitable for a temperature reconstruction. In this C-IT record from Lake Uddelermeer, we identified a RWP, a DACP and the MCA. The RWP is placed in the period from 2240-1760 cal. yr. BP, the DACP starts at 1760 cal. yr. BP and the MCA starts at 1280 cal. yr. BP. Our detailed summer temperature record shows that the average temperature drops by 1.5°C from the RWP to the DACP. Overall the temperature reconstructions appears to be too high, however, the trends, temperature fluctuations and timing of the cold and warm periods in this records are in agreement with other records and reconstructions indicating that the Uddelermeer record can be used as an representative record for temperature in the Netherlands during the first millennium AD.

Acknowledgements

This work is part of the project “The Dark Age of the Lowlands in an interdisciplinary light: people, landscape and climate in the Netherlands between AD 300 and 1000’ (NWO, section Humanities; 2012-2019: 360-60-110; www.darkagesproject.com). Loss on Ignition measurements were executed by T. Winkels and an initial low-resolutions set of chironomid samples were analysed by M. Wolma. The chironomid data was transferred to a temperature reconstruction by O. Heiri. We thank Keith Barber, who sadly passed away, for providing the chironomid data of Bigland Tarn and Talkin Tarn. The authors would like to thank H. Middelkoop and O. Heiri for useful comments on the paper. We thank T. Poelen and Kroondomein Het Loo for granting access to the site.

References

AHN Actueel Hoogtebestand Nederland. www.ahn.nl; www.nationaalgeoregister.nl.

Archeologisch Basis Register (ABR) in Nationale Onderzoeksagenda Archeologie (NOaA). (2016) Rijksdienst Cultureel Erfgoed. https://archeologieinnederland.nl/bronnen-en-kaarten/noaa. Accessed 01-08-2018

Axford Y., Geirsdóttir Á., Miller G.H., Langdon P.G. (2009) Climate of the Little Ice Age and the past 2000 years in northeast Iceland inferred from chironomids and other lake sediment proxies. Journal of Paleolimnology 41:7-24 doi:https://doi-org.proxy.library.uu.nl/10.1007/s10933-008-9251-1

Bajolle L., Larocque-Tobler I., Gandouin E., Lavoie M., Bergeron Y., Ali A.A. (2018) Major postglacial summer temperature changes in the central coniferous boreal forest of Quebec (Canada) inferred using chironomid assemblages. Journal of Quaternary Science 33:409-420 doi:https://doi.org/10.1002/jqs.3022

Barber K., Brown A., Langdon P., Hughes P. (2013) Comparing and cross-validating lake and bog palaeoclimatic records: A review and a new 5,000 year chironomid-inferred temperature record from northern England. Journal of Paleolimnology 49:497-512 doi:https://doi-org.proxy.library.uu.nl/10.1007/s10933-012-9656-8

Beug H.-J. (2004) Leitfaden der pollenbestimmung, für Mitteleuropa und angrenzende Gebiete. Fischer, Stuttgart:542 p.

Birks H.J.B. (1998) Numerical tools in palaeolimnology-Progress, potentialities, and problems. Journal of Paleolimnology 20:307-332

Birks H.J.B., Ter Braak C.J.F., Line J.M., Juggins S., Stevenson A.C. (1990) Diatoms and pH reconstruction. Phil Trans R Soc Lond B 327:263-278

611 Bohncke S.J.P. (1999) Verslag betreffende het onderzoek naar de archiefwaarde van de sedimenten van het
612 Uddelermeer. Vrije Universiteit Amsterdam, Amsterdam
613 Brodin Y.W. (1986) The postglacial history of Lake Flarken, southern Sweden, interpreted from subfossil insect
614 remains. Internationale Revue der gesamten Hydrobiologie und Hydrographie 71:371-432
615 Bronk Ramsey C. (2009) Bayesian analysis of radiocarbon dates. Radiocarbon 51:337-360
616 Brooks S.J., Axford Y., Heiri O., Langdon P.G., Larocque-Tobler I. (2012) Chironomids can be reliable proxies for
617 Holocene temperatures. A comment on Velle et al. (2010). The Holocene 22:1495-1500 doi:https://doi-
618 org.proxy.library.uu.nl/10.1177/0959683612449757
619 Brooks S.J., Birks H.J.B. (2000) Chironomid-inferred late-glacial and early-Holocene mean July air temperatures
620 for Kråkenes Lake, western Norway. Journal of Paleolimnology 23:77-89
621 Brooks S.J., Langdon P.G., Heiri O. (2007) The indentification and use of Palaeartic Chironomidae larvae in
622 palaeoecology. QRA Technical guide No. 10. Quaternary Research Association, London
623 Bunnik F.P.M. (1999) Vegetationsgeschichte der Lößbörden zwischen Rhein und Maas von der Bronzezeit bis in
624 die frühe Neuzeit., Utrecht University
625 Büntgen U., Myglan V.S., Ljungqvist F.C., McCormick M., Di Cosmo N., Sigl M., Jungclaus J., Wagner S., Krusic
626 P.J., Esper J. (2017) Reply to 'Limited Late Antique cooling'. Nature Geoscience 10:243
627 Büntgen U., Myglan V.S., Ljungqvist F.C., McCormick M., Di Cosmo N., Sigl M., Jungclaus J., Wagner S., Krusic
628 P.J., Esper J., Kaplan J.O., de Vaan M.A.C., Luterbacher J., Wacker L., Tegel W., Kirdyanov A.V. (2016)
629 Cooling and societal change during the Late Antique Little Ice Age from 536 to around 660 AD. Nature
630 Geosci 9:231-236 doi:https://doi.org/10.1038/NGEO2652
631 Büntgen U., Tegel W., Nicolussi K., McCormick M., Frank D., Trouet V., Kaplan J.O., Herzig F., Heussner K.U.,
632 Wanner H., Luterbacher J., Esper J. (2011) 2500 years of European climate variability and human
633 susceptibility. Science 331:578-582 doi:https://doi.org/10.1126/science.1197175
634 Cohen K.M., Toonen W.H.J., Weerts H.J.T. (2016) Overstromingen van de Rijn gedurende het Holocene
635 Relevantie van de grootste overstromingen voor archeologie van het Nederlands rivierengebied.
636 Deltares
637 Dalton C., Birks H.J.B., Brooks S.J., Cameron N.G., Evershed R.P., Peglar S.M., Scott J.A., Thompson R. (2005)
638 A multi-proxy study of lake-development in response to catchment changes during the Holocene at
639 Lochnagar, north-east Scotland. Palaeogeography, Palaeoclimatology, Palaeoecology 221:175-201
640 doi:https://doi.org/10.1016/j.palaeo.2005.02.007
641 Dörfler W., Feeser I., van den Bogaard C., Dreibrodt S., Erlenkeuser H., Kleinmann A., Merkt J., Wiethold J.
642 (2012) A high-quality annually laminated sequence from Lake Belau, Northern Germany: revised
643 chronology and its implications for palynological and tephrochronological studies The Holocene 22:1413-
644 1426 doi: https://doi.org/10.1177/0959683612449756
645 Engels S., Bakker M.A.J., Bohncke S.J.P., Cerli C., Hoek W.Z., Jansen B., Peters T., Renssen H., Sachse D., van
646 Aken J.M. (2016) Centennial-scale lake-level lowstand at Lake Uddelermeer (The Netherlands) indicates
647 changes in moisture source region prior to the 2.8-kyr event. The Holocene 26:1075-1091 doi:https://doi-
648 org.proxy.library.uu.nl/10.1177/0959683616632890
649 Engels S., Bohncke S.J.P., Bos J.A.A., Heiri O., Vandenberghe J., Wallinga J. (2008a) Environmental inferences
650 and chironomid-based temperature reconstructions from fragmentary records of the Weichselian Early
651 Glacial and Pleniglacial periods in the Niederlausitz area (eastern Germany). Palaeogeography,
652 Palaeoclimatology, Palaeoecology 260:405-416 doi:https://doi.org/10.1016/j.palaeo.2007.12.005
653 Engels S., Bohncke S.J.P., Heiri O., Nyman M. (2008b) Intraregional variability in chironomid-inferred temperature
654 estimates and the influence of river inundations on lacustrine chironomid assemblages. Journal of
655 Paleolimnology 40:129-142 doi:https://doi-org.proxy.library.uu.nl/10.1007/s10933-007-9147-5

Engels S., Cwynar L.C. (2011) Changes in fossil chironomid remains along a depth gradient: evidence for common faunal thresholds within lakes. Hydrobiologia 665:15-38 doi:https://doi-org.proxy.library.uu.nl/10.1007/s10750-011-0601-z

Engels S., Cwynar L.C., Rees A.B.H., Shuman B.N. (2012) Chironomid-based water depth reconstructions: an independant evaluation of site-specific and local interference models. Journal of Palaeolimology doi:https://doi-org.proxy.library.uu.nl/10.1007/s10933-012-9638-x

Engels S., Self A.E., Luoto T.P., Brooks S.J., Helmens K.F. (2014) A comparison of three Eurasian chironomid-climate calibration datasets on a W-E continentality gradient and the implications for quantitative temperature reconstructions. Journal of Paleolimnology 51:529-547 doi:https://doi-org.proxy.library.uu.nl/10.1007/s10933-014-9772-8

Engels S., van Oostrom R., Cherli C., Dungait J.A.J., Jansen B., van Aken J.M., van Geel B., Visser P.M. (2018) Natural and anthropogenic forcing of Holocene lake ecosystem development at Lake Uddelermeer (The Netherlands). Journal of Paleolimnology 59:329-347 doi:https://doi-org.proxy.library.uu.nl/10.1007/s10933-017-0012-x

Erkens G. (2009) Sediment dynamics in the Rhine catchement-Quantification of fluvial response to climate change and human impact. Netherlands Geographical Studies 388

Faegri K., Iversen J. (1989) Textbook of Pollen Analysis, revised by Faegri K, Kaland PE, Krzywinski K. J Wiley, New York

Farmer A.M., Spence D.H.N. (1986) The growth strategies and distribution of isoetids in Scottish freshwater lochs. Aquatic Botany 26:247-258

Gräslund B., Price N. (2012) Twilight of the gods? The ‘dust veil event’ of AD 536 in critical perspective Antiquity 86:428-443 doi:doi:10.1017/S0003598X00062852

Grimm E.C. (1991-2015) Tilia., 2.0.41 edn.,

Groenewoudt B.J., Schut P.A.C., van der Heijden F.J.G., Peeters H., Wispelwey M.H. (2006) Een inventariserend veldonderzoek bij de Hunneschans (Uddel, Gelderland): nieuwe gegevens over de steentijdbewoning bij het Uddelermeer en een beknopt overzicht van de onderzoeksgeschiedenis van de Hunneschans: Rapportage Archeologische Monumentenzorg 143.

Groenewoudt B.J., van Lanen R.J. (2018) Diverging decline. Reconstructing and validating (post-)Roman population trends (AD 0-1000) in the Rhine-Meuse delta (the Netherlands). Post Classical Archaeologies 8:30

Hannon G.E., Gaillard M.-J. (1997) The plant-macrofossil record of past lake-level changes. Journal of Paleolimnology 18:15-28

Heidinga H.A. (1987) Medieval Settlement and Economy North of the Lower Rhine: Archeology and History of Kootwijk and the Veluwe (the Netherlands). Van Gorcum Ltd,

Heiri O., Brooks S.J., Birks H.J.B., Lotter A.F. (2011) A 274-lake calibration data-set and inference model for chironomid-based summer air temperature reconstruction in Europe. Quaternary Science Reviews 30:3445-3456 doi:https://doi.org/10.1016/j.quascirev.2011.09.006

Heiri O., Brooks S.J., Renssen H., Bedford A., Hazekamp M., Ilyashuk B., Jeffers E.S., Lang B., Kirilova E., Kuiper S. (2014) Validation of climate model-inferred regional temperature change for late-glacial Europe. Nature communications 5:4914 doi:https://doi.org/10.1038/ncomms5914

Heiri O., Lotter A.F., Lemcke G. (2001) Loss on ignition as a method for estimating organic and carbonate content in sediments: reproducibility and comparability of results. Journal of Paleolimnology 25:101-110

Helama S., Jones P.D., Briffa K.R. (2017a) Dark Ages Cold Period: A literature review and directions for future research. The Holocene 27:1600-1606 doi:https://doi.org/10.1177/0959683617693898

Helama S., Jones P.D., Briffa K.R. (2017b) Limited Late Antique cooling. Nature Geoscience 10:242

Jansma E., Gouw-Bouman M.T.I.J., Van Lanen R.J., Pierik H.J., Cohen K.M., Groenewoudt B.J., Hoek W.Z., Stouthamer E., Middelkoop H. (2014) The Dark Age of the Lowlands in an interdisciplinary light: people, landscape and climate in The Netherlands between AD 300-1000. European Journal of Post-Classical Archaeologies (PCA 4):471-476

Kalis A.J., Karg S., Meurers-Balke H., Teunissen-van OOrschot H. (2008) Mensch und Vegetation am Unteren Niederrhein währen der Eisen- und Römerzeit. In: Müller M, Schalles H-J, Zieling N (eds) Colonia Ulpia Traiana, Xanten und sein Umland in römischer Zeit, Xantener Berichte, Geschichte der Stadt Xanten., vol 1. pp 31-48

Knol E. (1993) De Noordnederlandse kustlanden in de Vroege Middeleeuwen., VU University Amsterdam

Kraanen C.J.M., Pape J.C. (1965) De bodemgesteldheid van de omgeving van het Uddelermeer. STIBOKA,

Langdon P.G., Barber K.E., Lomas-Clarke S.H. (2004) Reconstructing climate and environmental change in northern England through chironomid and pollen analyses: evidence from Talkin Tarn, Cumbria. Journal of Palaeolimology 32:197-203

Langdon P.G., Ruiz Z., Brodersen K.P., Foster I.D.L. (2006) Assessing lake eutrophication using chironomids: understanding the nature of community response in different lake types. Freshwater biology 51:562-577 doi:https://doi.org/doi:10.1111/j.1365-2427.2005.01500.x

Larsen L.B., Vinther B.M., Briffa K.R., Melvin T.M., Clausen H.B., Jones P.D., Siggaard-Andersen M.L., Hammer C.U., Eronen M., Grudd H., Gunnarson B.E., Hantemirov R.M., Naurzbaev M.M., Nicolussi K.C.L. (2008) New ice core evidence for a volcanic cause of the A.D. 536 dust veil. Geophysical Research Letters 35:n/a-n/a doi:https://doi-org.proxy.library.uu.nl/10.1029/2007GL032450

Litt T., Schölzel C., Kühl N., Brauer A. (2009) Vegetation and climate history in the Westeifel Volcanic Field (Germany) during the past 11 000 years based on annually laminated lacustrine maar sediments. Boreas 38:679-690 doi:https://doi.org/10.1111/j.1502-3885.2009.00096.x

Ljungqvist F.C. (2009) Temperature proxy records covering the last two millennia: a tabular and visual overview. Geografiska Annaler: Series A, Physical Geography 91:11-29 doi:https://doi.org/10.1111/j.1468-0459.2009.00350.x

Ljungqvist F.C. (2010) A new reconstruction of temperature variability in the extra-tropical northern hemisphere during the last two millennia. Geografiska Annaler, series A:339-351

Luoto T.P. (2011) The relationship between water quality and chironomid distribution in Finland—a new assemblage-based tool for assessments of long-term nutrient dynamics. Ecological Indicators 11:255-262 doi:https://doi.org/10.1016/j.ecolind.2010.05.002

Luoto T.P. (2012) Intra-lake patterns of aquatic insect and mite remains. Journal of Paleolimnology 47:141-157 doi:https://doi-org.proxy.library.uu.nl/10.1007/s10933-011-9565-2

McCormick M., Büntgen U., Cane M.A., Cook E.R., Harper K., Huybers P., Litt T., Manning S.W., Mayewski P.A., More A.F.M., Nicolussi K., Tegel W. (2012) Climate Change during and after the Roman Empire: Reconstructing the Past from Scientific and Historical Evidence. Journal of Interdisciplinary History 43:169-220

McKeown M., Potito A.P. (2016) Assessing recent climatic and human influences on chironomid communities from two moderately impacted lakes in western Ireland. Hydrobiologia 765:245-263 doi:https://doi-org.proxy.library.uu.nl/10.1007/s10750-015-2418-7

Millet L., Arnaud F., Heiri O., Magny M., Verneaux V., Desmet M. (2009) Late-Holocene summer temperature reconstruction from chironomid assemblages of Lake Anterne, northern French Alps. The Holocene 19:317-328 doi:https://doi.org/10.1177/0959683608100576

Moller Pillot H.K.M. (1984a) De Larven der Nederlandse Chironomidae (Diptera): Orthocladiinae sensu lato. Nederlandse Faunistische Mededelingen 1:1-175

Moller Pillot H.K.M. (1984b) De larven der Nederlandse Chironomidae (Diptera); (Inleiding, Tanypodinae & Chironomini). Nederlandse Faunistische Mededelingen 1:1-277

Moller Pillot H.K.M. (2013) Chironomidae Larvae of the Netherlands and adjacent lowlands: biology and ecology of the chironomini. KNNV publishing,

Moller Pillot H.K.M., Klink A.G. (2009) Chironomidae larvae. Biology and Ecology of the Chironomini KNNV Publishing, Zeist

Moore P.D., Webb J.A., Collison M.E. (1991) Pollen analysis. Blackwell scientific publications,

Nazarova L., de Hoog V., Hoff U., Dirksen O., Diekmann B. (2013) Late Holocene climate and environmental changes in Kamchatka inferred from the subfossil chironomid record. Quaternary Science Reviews 67:81-92 doi:https://doi.org/10.1016/j.quascirev.2013.01.018

Padisák J., Krienitz L., Scheffler W., Koschel R., Kristiansen J., Grigorszky I. (1998) Phytoplankton succession in the oligotrophic Lake Stechlin (Germany) in 1994 and 1995 Hydrobiologia 369:179-197

Pierik H.J. (2017) Past human-landscape interactions in the Netherlands: Reconstructions from sand belt to coastal-delta plain for the first millennium AD. vol 139. Utrecht studies in earth sciences. Utrecht University,

Pierik H.J., Cohen K.M., Stouthamer E. (2016) A new GIS approach for reconstructing and mapping dynamic late Holocene coastal plain palaeogeography. Geomorphology 270:55-70 doi:http://dx.doi.org/10.1016/j.geomorph.2016.05.037

Pierik H.J., Stouthamer E., Cohen K.M. (2017) Natural levee evolution in the Rhine-Meuse delta, the Netherlands, during the first millennium CE. Geomorphology 295:215-234 doi:https://doi.org/10.1016/j.geomorph.2017.07.003

Pierik H.J., van Lanen R.J. (2017) Roman and early-medieval habitation patterns in a delta landscape: The link between settlement elevation and landscape dynamics. Quaternary International doi:https://doi.org/10.1016/j.quaint.2017.03.010

Pierik H.J., Van Lanen R.J., Gouw-Bouman M.T.I.J., Groenewoudt B., Wallinga J., Hoek W.Z. (2018) Controls on late Holocene drift-sand dynamics: the role of people and climate on inland aeolian activity in the Netherlands The Holocene 28:1361-1381 doi:https://doi.org/10.1177/0959683618777052

Koomen A., Maas G. (2004) Geomorfologische Kaart Nederland (GKN); Achtergronddocument bij het landsdekkende digitale bestand. Alterra.

Polak B. (1959) Palynology of the “Uddeler Meer”. A Contribution to our Knowledge of the Vegetation and of the Agriculture in the Northern Part of the Veluwe in Prehistoric and Early Historic Times. Acta botanica neerlandica 8:547-571

Potito A.P., Woodward C.A., McKeown M., Beilman D.W. (2014) Modern influences on chironomid distribution in western Ireland: potential for palaeoenvironmental reconstruction. Journal of Paleolimnology 52:385-404 doi:https://doi-org.proxy.library.uu.nl/10.1007/s10933-014-9800-8

Punt W., Blackmore S., Clarke G.C.S. (1976) The Northwest European pollen flora 1. Elsevier, Amsterdam

Punt W., Blackmore S., Clarke G.C.S. (1980) The Northwest European pollen flora 2. Elsevier, Amsterdam

Punt W., Blackmore S., Clarke G.C.S. (1981) The Northwest European pollen flora 3. Elsevier, Amsterdam

Punt W., Blackmore S., Clarke G.C.S. (1984) The Northwest European pollen flora 4. Elsevier, Amsterdam

Punt W., Blackmore S., Clarke G.C.S. (1988) The Northwest European pollen flora 5. Elsevier, Amsterdan=m

Punt W., Blackmore S., Clarke G.C.S. (1991) The Northwest European pollen flora 6. Elsevier,

Punt W., Blackmore S., Clarke G.C.S. (1995) The Northwest European pollen flora 7. Elsevier,

Punt W., Blackmore S., Hoen P.P., Stafford P.J. (2003) The Northwest European pollen flora 8. Elsevier, Amsterdam

790 Rasmussen S.O., Andersen K.K., Svensson A.M., Steffensen J.P., Vinther B.M., Clausen H.B., Siggaard-
791 Andersen M.L., Johnsen S.J., Larsen L.B., Dahl-Jensen D., Bigler M., Röthlisberger R., Fischer H.,
792 Goto-Azuma K., Hansson M.E., Ruth U. (2006) A new Greenland ice core chronology for the last glacial
793 termination. Journal of Geophysical Research: Atmospheres 111:n/a-n/a doi:10.1029/2005jd006079
794 Riechelmann D., Gouw-Bouman M.T.I.J. (2019) Climate during the first millennium AD in NW Europe: a review of
795 climate reconstructions from terrestrial archives. Quaternary Research 91:111-131
796 doi:https://doi.org/10.1017/qua.2018.84
797 Rieradevall M., Brooks S.J. (2001) An identification guide to subfossil Tanypodinae larvae (Insecta: Diptera:
798 Chrironomidae) based on cephalic setation. Journal of Paleolimnology 25:81-99
799 Roelofs J.G.M., Schuurkes J.A.A.R., Smits A.J.M. (1984) Impact of acidification and eutrophication on
800 macrophyte communities in soft waters. II. Experimental studies. Aquatic Botany 18:389-411
801 Rørslett B., Brettum P. (1989) The genus Isoëtes in Scandinavia: an ecological review and perspectives. Aquatic
802 Botany 35:223-261
803 Sand-Jensen K. (1978) Metabolic adaptation and vertical zonation of Littorella uniflora (L.) Aschers. and Isoetes
804 lacustris L. Aquatic Botany 4:1-10
805 Sohl H. (1983) A palaeo-ecological investication of the Late Glacial and Holocene lake sediments of the
806 Uddelermeer (The Netherlands): methods and some provisional results. Quaternary studies in Poland
807 9:547-571
808 Stouthamer E., Berendsen H.J.A. (2000) Factors Controlling the Holocene Avulsion History of the Rhine-Meuse
809 Delta (The Netherlands). Journal of Sedimentary Research 70:1051-1064 doi:10.1306/033000701051
810 Taylor K.J., McGinley S., Potito A.P., Molloy K., Beilman D.W. (2018) A mid to late Holocene chironomid-inferred
811 temperature record from northwest Ireland. Palaeogeography, Palaeoclimatology, Palaeoecology
812 505:274-286 doi:https://doi.org/10.1016/j.palaeo.2018.06.006
813 Taylor K.J., Potito A.P., Beilman D.W., Ghilardi B., O'Connell M. (2013) Palaeolimnological impacts of early
814 prehistoric farming at Lough Dargan, County Sligo, Ireland. Journal of Archaeological Science 40:3212-
815 3221 doi:https://doi.org/10.1016/j.jas.2013.04.002
816 Taylor K.J., Potito A.P., Beilman D.W., Ghilardi B., O'Connell M. (2017a) Impact of early prehistoric farming on
817 chironomid communities in northwest Ireland. Journal of Paleolimnology 57:227-244
818 doi:https://doi.org/10.1007/s10933-017-9942-6
819 Taylor K.J., Stolze S., Beilman D.W., Potito A.P. (2017b) Response of chironomids to Neolithic land-use change
820 in north-west Ireland. The Holocene 27:879-889 doi:https://doi.org/10.1177/0959683616675935
821 Telford R.J., Birks H.J.B. (2011) A novel method for assessing the statistical significance of quantitative
822 reconstructions inferred from biotic assemblages. Quaternary Science Reviews 30:1272-1278
823 doi:https://doi.org/10.1016/j.quascirev.2011.03.002
824 ter Braak C.J.F., Šmilauer P. (2012) Canoco reference manual and user's guide: software for ordination, version
825 5.0. Microcomputer power,
826 Teunissen D. (1990) Palynologisch onderzoek in het oostelijk rivierengebied: een overzicht. In: Mededelingen van
827 de afdeling Biogeologie van de Discipline Biologie van de Katholieke Universiteit van Nijmegen. p 16
828 Tinner W., Lotter A.F., Ammann B., Conedera M., Hubschmid P., van Leeuwen J.F.N., Wehrli M. (2003) Climatic
829 change and contemporaneous land-use phases north and south of the Alps 2300 BC to 800 AD.
830 Quaternary Science Reviews 22:1447-1460 doi:https://doi.org/10.1016/S0277-3791(03)00083-0
831 Toohey M., Krüger K., Sigl M., Stordal F., Svensen H. (2016) Climatic and societal impacts of a volcanic double
832 event at the dawn of the Middle Ages Climatic Change 136:401-412
833 Toonen W.H.J. (2013) A Holocene flood record of the Lower Rhine. Utrecht University

834 Vallenduuk H.J., Moller Pillot H.K.M. (2007) Chironomidae larvae of the Netherlands and adjacent lowlands.
835 KNNV Publishing,
836 van Asch N. (2012) Environmental response to Lateglacial climate change-Reconstructions of temperature and
837 vegetation changes in northwest Europe., Utrecht University
838 van Geel B. (1972) Palynology of a section from the raised bog 'Wietmarscher moor', with special reference to
839 fungal remains. Plant Biology 21:261-284
840 van Geel B. (1978) A palaeoecological study of Holocene peat bog sections in Germany and the Netherlands,
841 based on the analysis of pollen, spores and macro-and microscopic remains of fungi, algae,
842 cormophytes and animals. Review of Palaeobotany and Palynology 25:1-120
843 van Geel B., Buurman J., Brinkkemper O., Schelvis J., Aptroot A., van Reenen G., Hakbijl T. (2003)
844 Environmental reconstruction of a Roman Period settlement site in Uitgeest (The Netherlands), with
845 special reference to coprophilous fungi. Journal of Archaeological Science 30:873-883
846 doi:https://doi.org/10.1016/S0305-4403(02)00265-0
847 Vinther B.M., Clausen H.B., Johnsen S.J., Rasmussen S.O., Andersen K.K., Buchardt S.L., Dahl-Jensen D.,
848 Seierstad I.K., Siggaard-Andersen M.L., Steffensen J.P., Svensson A., Olsen J., Heinemeier J. (2006) A
849 synchronized dating of three Greenland ice cores throughout the Holocene. Journal of Geophysical
850 Research: Atmospheres 111 doi:10.1029/2005jd006921
851 Vos P.C., Van Heeringen R.M. (1997) Holocene geology and occupation history of the Province of Zeeland
852 Mededelingen Nederlands Instituut voor Toegepaste Geowetenschappen TNO 59:5-109
853 Wanner H., Beer J., Bütikofer J., Crowley T.J., Cubasch U., Flückiger J., Goosse H., Grosjean M., Joos F.,
854 Kaplan J.O., Küttel M., Müller S.A., Prentice I.C., Solomina O., Stocker T.F., Tarasov P., Wagner M.,
855 Widmann M. (2008) Mid- to Late Holocene climate change: an overview. Quaternary Science Reviews
856 27:1791-1828 doi:http://dx.doi.org/10.1016/j.quascirev.2008.06.013
857 Wanner H., Solomina O., Grosjean M., Ritz S.P., Jetel M. (2011) Structure and origin of Holocene cold events.
858 Quaternary Science Reviews 30:3109-3123
859 Weeda E.J., Schaminée J.H.J., Van Duuren L. (2000) Atlas van Plantengemeenschappen in Nederland. deel 1:
860 Wateren, moerassen en natte heiden. KNNV Uitgeverij, Utrecht
861 Weeda E.J., Westra R., Westra C., Westra T. (1988) Nederlandse oecologische flora, wilde planten en hun
862 relaties. deel 3. Hilversum
863 Wiederholm T. (1983) Chironomidae of Holarctic region: keys and diagnoses. Part 1. Larvae Entomol Scand
864 Suppl 19:1-457

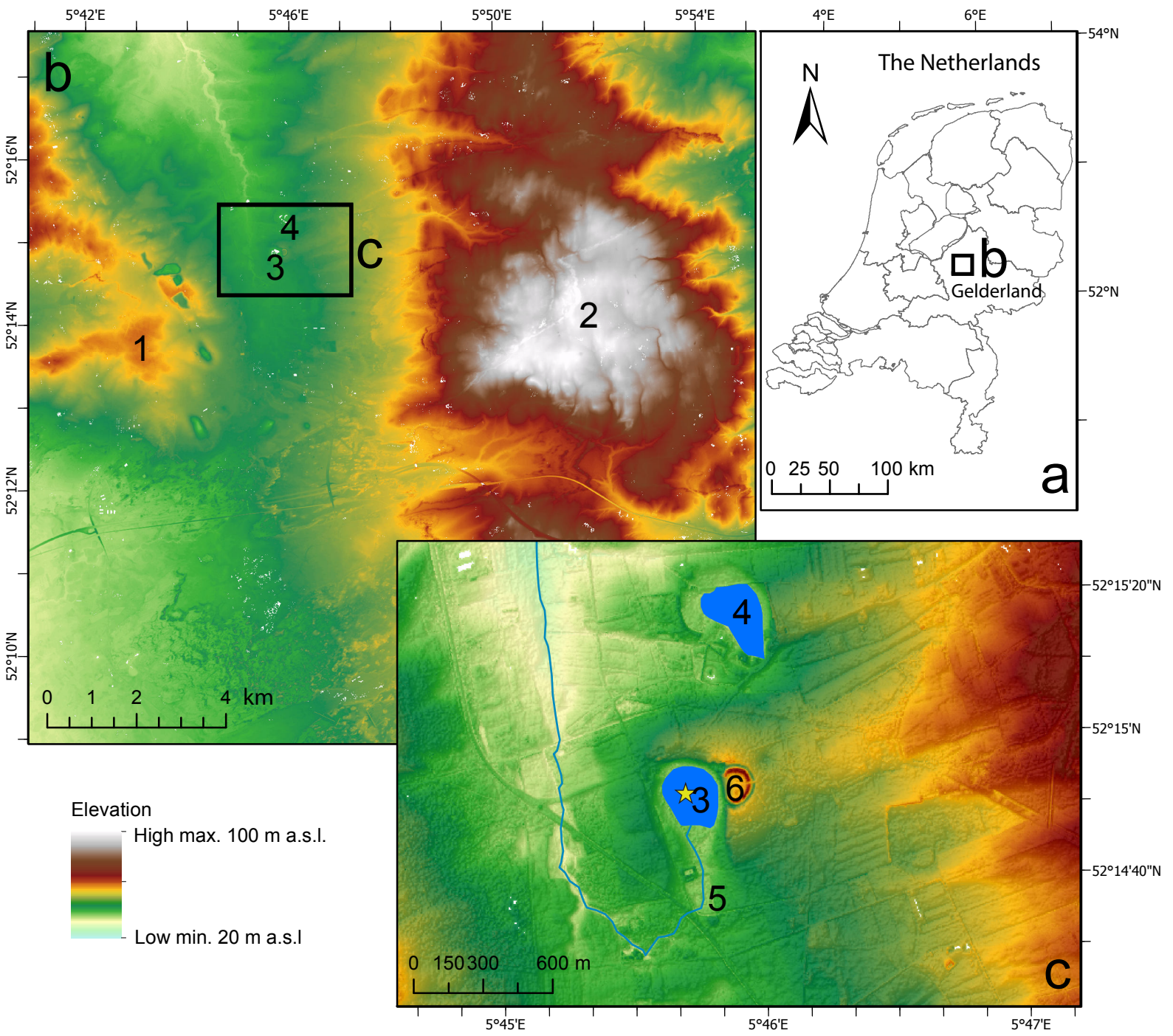
5°42'E
5°46'E
5°50'E
5°54'E
4°E
6°E
54°N
52°N
52°16'N
52°14'N
52°12'N
52°10'N
b
c
1
2
3
4
0 1 2 4 km
N
The Netherlands
b
Gelderland
0 25 50 100 km
a
52°15'20"N
52°15'N
52°14'40"N
5
6
0 150 300 600 m
c
5°45'E
5°46'E
5°47'E
Elevation
High max. 100 m a.s.l.
Low min. 20 m a.s.l

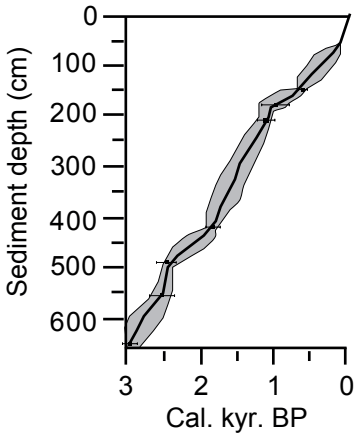
0
100
200
300
400
500
600
Sediment depth (cm)
3
2
1
0
Cal. kyr. BP

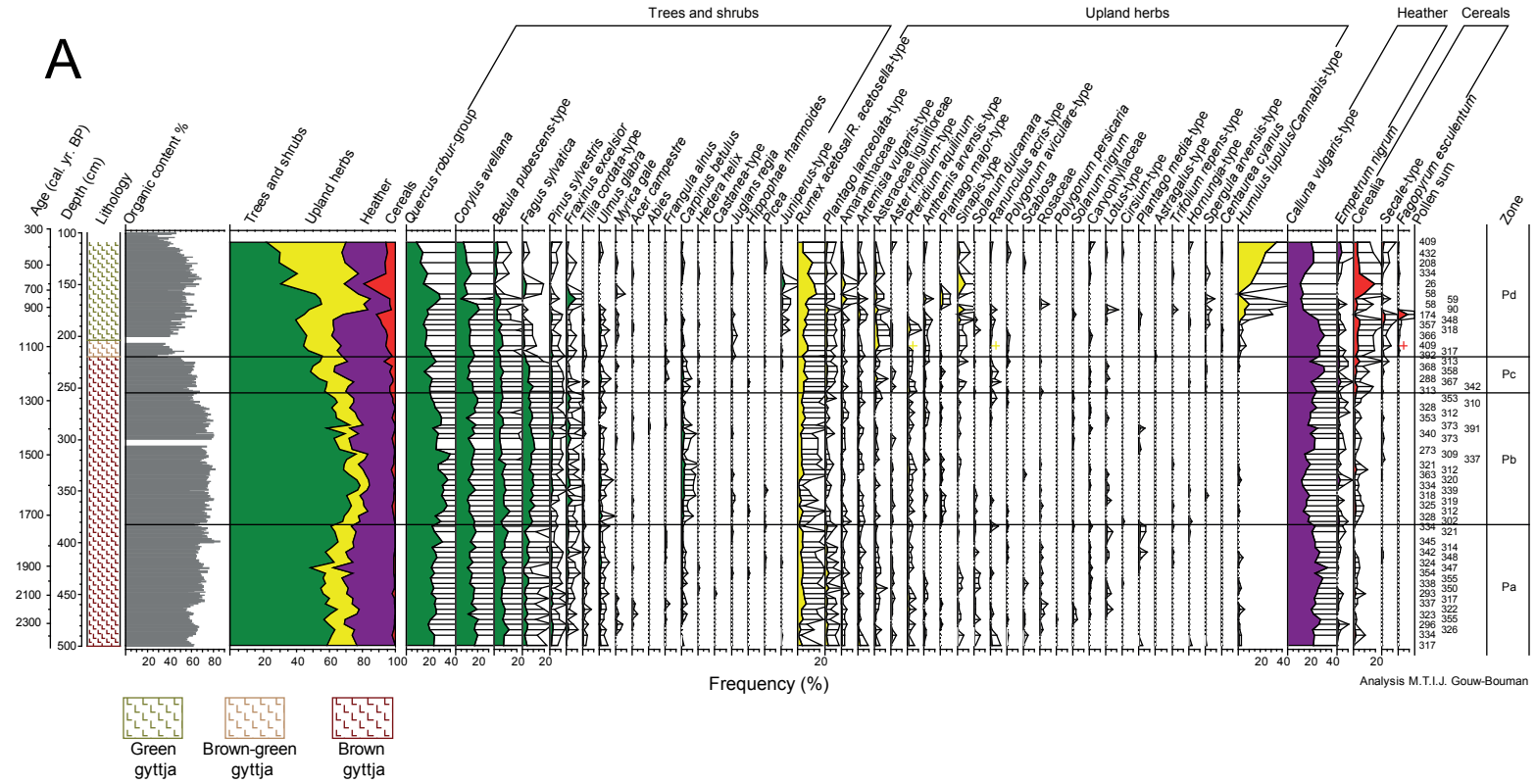
A
Trees and shrubs
Upland herbs
Heather
Cereals
Age (cal. yr. BP)
Depth (cm)
Lithology
Organic content %
Trees and shrubs
Upland herbs
Heather
Cereals
Quercus robur-group
Corylus avellana
Betula pubescens-type
Fagus sylvatica
Pinus sylvestris
Fraxinus excelsior
Ulmus glabra
Tilia cordata-type
Myrica gale
Acer campestre
Abies
Frangula alnus
Carpinus betulus
Hedera helix
Castanea-type
Juglans regia
Hippophaë rhamnoides
Picea
Juniperus-type
Rumex acetosa/R. acetosella-type
Plantago lanceolata-type
Amaranthaceae
Artemisia vulgaris-type
Asteraceae liguliflorae
Aster tripolium-type
Pteridium aquilinum
Antirrhinum arvensis-type
Plantago major-type
Sinapis-type
Solanum dulcamara
Ranunculus acris-type
Polygonum aviculare-type
Scabiosa
Rosaceae
Polygonum persicaria
Solanum nigrum
Caryophyllaceae
Lotus-type
Cirsium-type
Plantago media-type
Astragalus-type
Trifolium repens-type
Hornungia-type
Spergula arvensis-type
Centaurea cyanus
Humulus lupulus/Cannabis-type
Calluna vulgaris-type
Empetrum nigrum
Cerealia
Secale-type
Fagopyrum esculentum
Pollen sum
Zone
Pd
Pc
Pb
Pa
Frequency (%)
Analysis M.T.I.J. Gouw-Bouman
Green gyttja
Brown-green gyttja
Brown gyttja
B
Marsh and swamp
Aquatics
Fungi
Age (cal. yr. BP)
Depth (cm)
Lithology
Trees and shrubs
Upland herbs
Heather
Cereals
Alnus glutinosa-type
Salix
Poaceae
Cyperaceae
Sphagnum
Dryopteris
Polygonum amphibium-type
Potentilla-type
Ranunculaceae
Typha angustifolia-type
Filipendula
Hydrocotyle vulgaris
Typha latifolia-type
Ophioglossum-type
Isoëtes
Littorella uniflora-type
Nymphaea alba
HdV-type 127
Nuphar lutea
Potamogeton-type
Myriophyllum alterniflorum-type
Botryococcus
Pediastrum
Scenedesmus
Tetraedron minimum
HdV-type 128
Sordaria-type
Glomus
Sporormiella
Cercophora-type
Arnium imitans-type
Chaetomium
Podosporа-type
Cetlasmospora
Tripterospora-type
Charcoal
Zone
Pd
Pc
Pb
Pa
Frequency (%)
Analysis M.T.I.J. Gouw-Bouman
Green gyttja
Brown-green gyttja
Brown gyttja

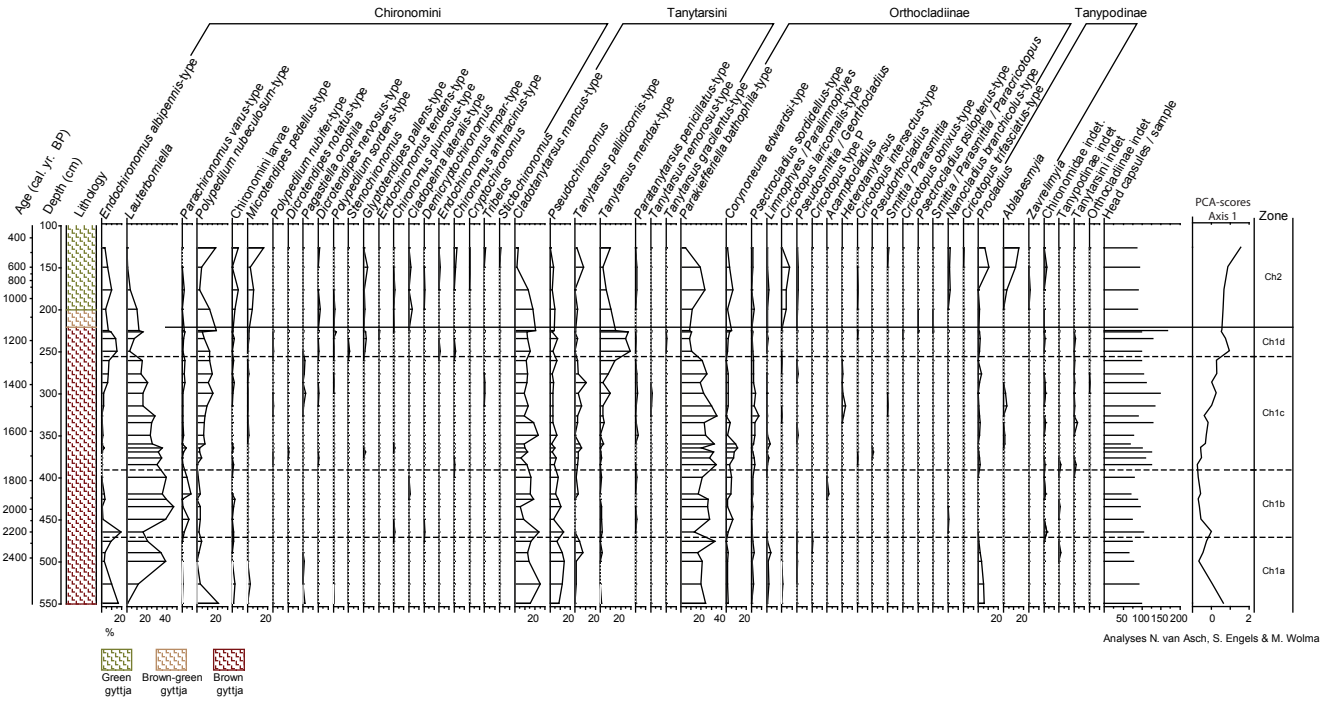
Chironomini
Tanytarsini
Orthocladiinae
Tanypodinae
Age (cal. yr. BP)
Depth (cm)
Lithology
Endochironomus albipennis-type
Lauterborniella
Parachironomus vanus-type
Polypedilum nubeculosum-type
Chironomini larvae
Microtendipes pedellus-type
Polypedilum nubifer-type
Dicrotendipes notatus-type
Paggastiella orophila
Dicrotendipes nervosus-type
Polypedilum scirpus-type
Stenochironomus
Glyptotendipes pallens-type
Glyptotendipes tendens-type
Chironomus plumosus-type
Cladopelma lateralis-type
Demicryptochironomus
Endochironomus impar-type
Chironomus anthracinus-type
Cryptochironomus
Tribelos
Stictochironomus
Cladotanytarsus mancus-type
Pseudochironomus
Tanytarsus pallidicornis-type
Tanytarsus mendax-type
Paratanytarsus penicillatus-type
Tanytarsus nemorosus-type
Tanytarsus gracilentus-type
Paratlantemella batophila-type
Corynoneura edwardsi-type
Psectrocladius sordidellus-type
Limnophyes / Paralimnophyes
Cricotopus / Paratrichocladius
Pseudosmittia / Georthocladius
Acamptocladius type P
Heterotanytarsus
Pseudorthocladius
Cricotopus intersectus-type
Smittia / Parasmittia
Cricotopus obnutus-type
Psectrocladius psilopterus-type
Smittia / Parasmittia / Paracricotopus
Nanocladius branchicolus-type
Cricotopus trifasciatus-type
Procladius
Ablabesmyia
Zavrelimyia
Chironomidae indet.
Tanypodinae indet.
Tanytarsini indet.
Orthocladiinae indet.
Head capsules / sample
PCA-scores
Axis 1
Zone
Ch2
Ch1d
Ch1c
Ch1b
Ch1a
%
Green gyttja
Brown-green gyttja
Brown gyttja
Analyses N. van Asch, S. Engels & M. Wolma

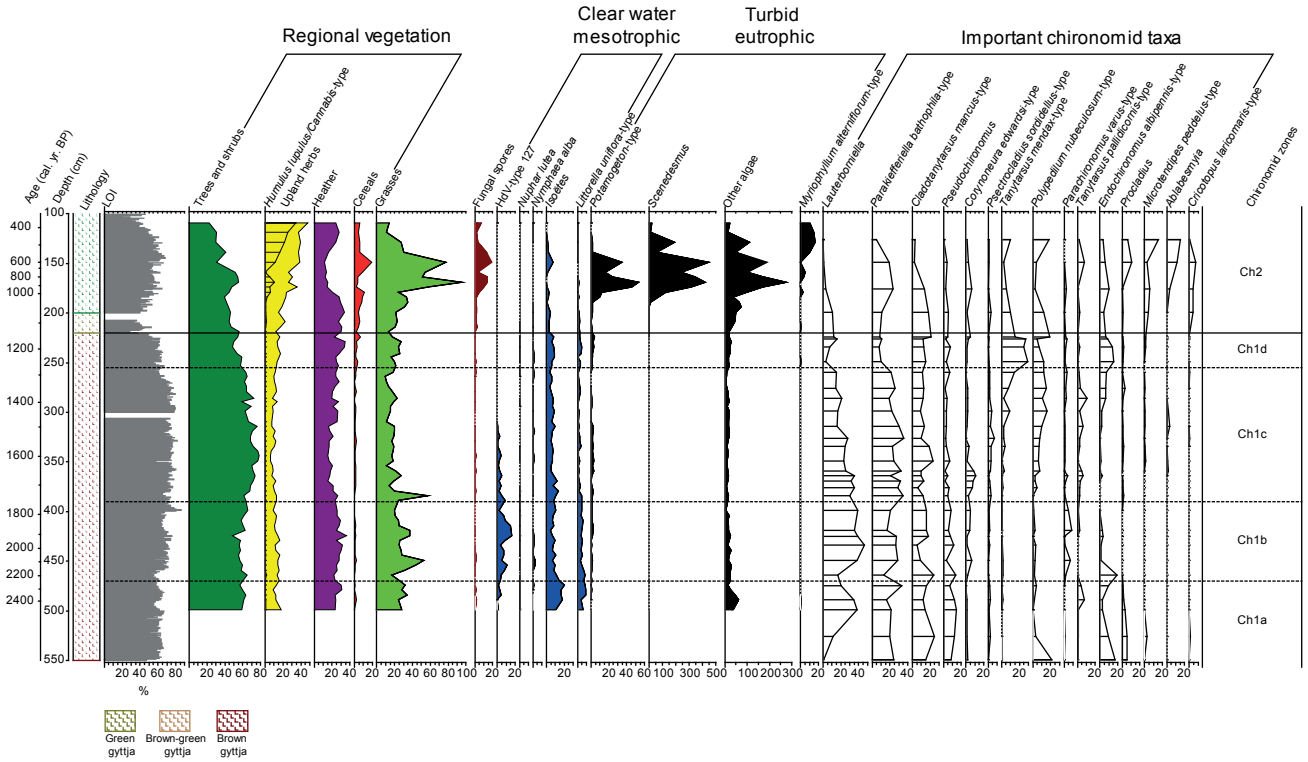
Regional vegetation
Clear water mesotrophic
Turbid eutrophic
Important chironomid taxa
Age (cal. yr. BP)
Depth (cm)
Lithology
LOI
Trees and shrubs
Humulus lupulus/Cannabis-type
Upland herbs
Heather
Cereals
Grasses
Fungal spores
HdV-type 127
Nuphar lutea
Nymphaea alba
Isoetes
Littorella uniflora-type
Potamogeton-type
Scenedesmus
Other algae
Myriophyllum alterniflorum-type
Lauterborniella
Parakiefferiella bathophilis-type
Cladotanytarsus mancus-type
Pseudochironomus
Corynoneura edwardsi-type
Psectrocladius sordidellus-type
Tanytarsus mendax-type
Polypedilum nubeculosum-type
Parachironomus varus-type
Tanytarsus pallidicornis-type
Endochironomus albipennis-type
Procladius
Microtendipes pedellus-type
Ablabesmyia
Cricotopus laricomalis-type
Chironomid zones
Ch2
Ch1d
Ch1c
Ch1b
Ch1a
%
Green gyttja
Brown-green gyttja
Brown gyttja

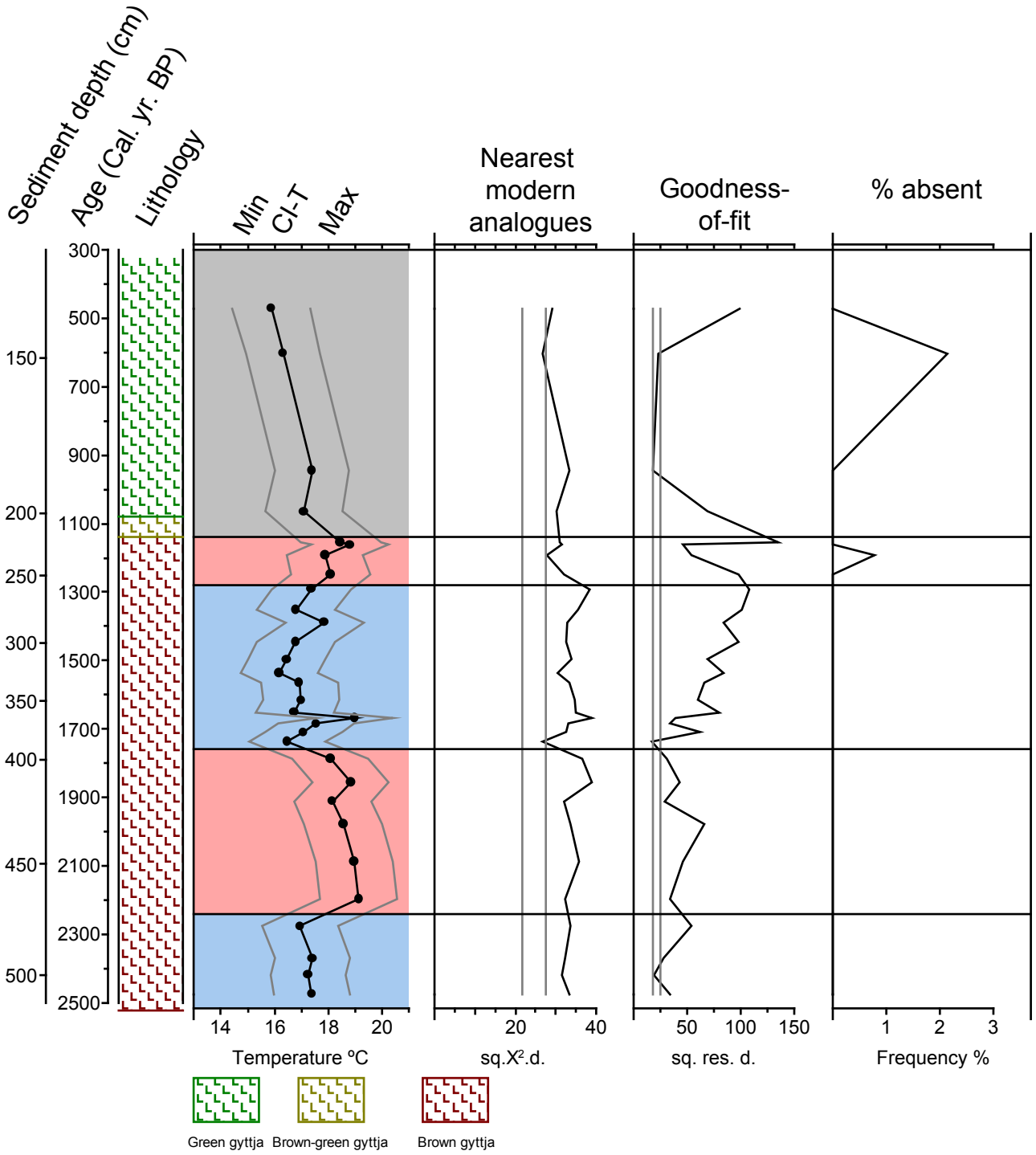
Sediment depth (cm)
Age (Cal. yr. BP)
Lithology
Min
Cl-T
Max
Nearest modern analogues
Goodness-of-fit
% absent
300
500
150
700
900
200
1100
250
1300
300
1500
350
1700
400
1900
450
2100
2300
500
2500
14
16
18
20
Temperature ºC
20
40
sq.X².d.
50
100
150
sq. res. d.
1
2
3
Frequency %
Green gyttja
Brown-green gyttja
Brown gyttja

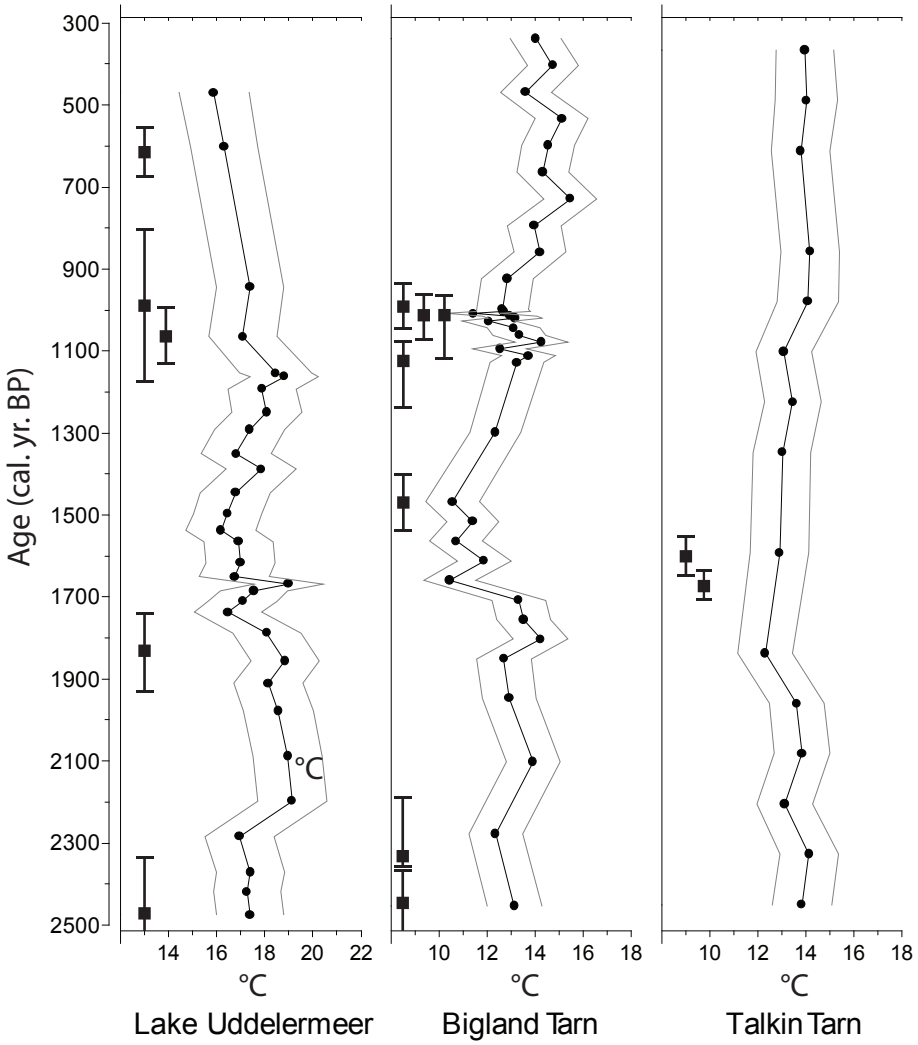
Age (cal. yr. BP)
300
500
700
900
1100
1300
1500
1700
1900
2100
2300
2500
°C
14
16
18
20
22
°C
Lake Uddelermeer
10
12
14
16
18
°C
Bigland Tarn
10
12
14
16
18
°C
Talkin Tarn

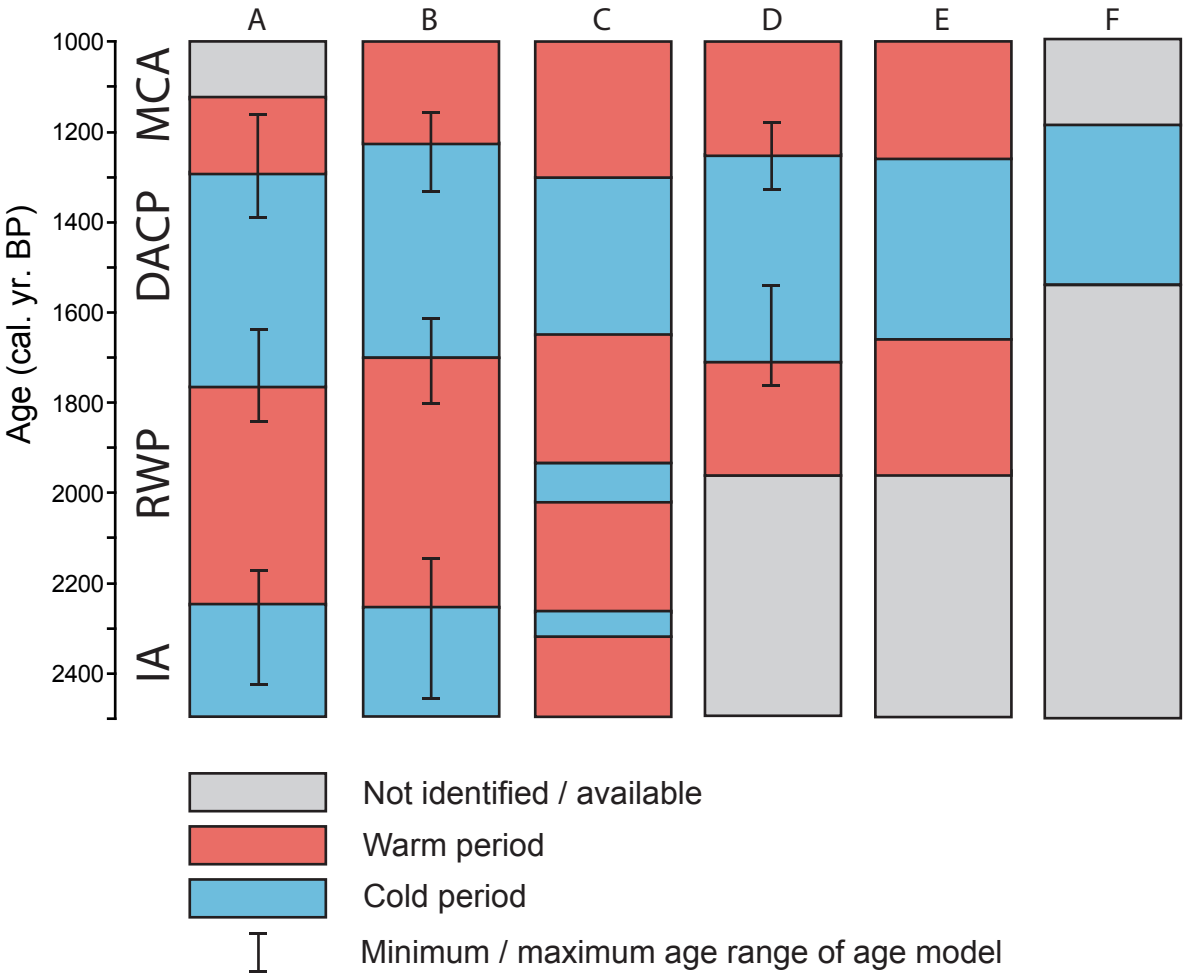
A
B
C
D
E
F
1000
1200
1400
1600
1800
2000
2200
2400
Age (cal. yr. BP)
MCA
DACP
RWP
IA
Not identified / available
Warm period
Cold period
Minimum / maximum age range of age model

Figure 1 (a) Location of Lake Uddelermeer; (b) Lidar elevation model of the central Netherlands (AHN; www.ahn.nl) and (c) the area directly surrounding Lake Uddelermeer. Yellow star indicates location core. Numbers indicate sites discussed in the text. 1 Ice pushed ridge Garderen-Ermelo max. 50 m A.S.L.; 2 Ice pushed ridge Apeldoorn max. 100 m A.S.L. ; 3 Lake Uddelemeer; 4 Lake Bleekemeer; 5 brook Leuvenemse beek; 6 medieval ringfort (ringwalburg) (Koomen & Maas, 2004; Heidinga, 1987). For visibility purposes (c) is plotted with a different colour range, only a relative elevation legend is shown for both maps.

Figure 2 Bayesian modelled age-depth model of core section 50 - 650 cm depth for central Core E from Lake Uddelermeer (figure adapted from Engels et al. (2016)). The 95% probability distribution range is shown in grey, calibrated C^{14} ages and 95% probability ranges are shown as black squares with error bars.

Figure 3 Percentage diagram of selected pollen, spores and NPPs from Lake Uddelermeer showing regional (A) and local (B) vegetation development in and around Lake Uddelermeer. All curves are shown with an additional fivefold exaggeration. Diagram plotted on sediment depth (cm) with a secondary scale (cal. yr. BP) plotted for comparison. Sedimentological and Loss-on-Ignition (represented as organic content% in 3A) profiles are plotted to the left of the pollen curves. The presence of charcoal (indicated with '+' present; '++' present in large quantities) is plotted to the right of the pollen curves.

Figure 4 Percentage diagram showing all chironomid taxa and the chironomid count sum (head capsules/ sample) for Lake Uddelermeer. Diagram plotted on sediment depth (cm) with a secondary scale (cal. yr. BP) plotted for comparison. The sedimentological profile is plotted to the left of the chironomid curves. To the right the scores of the chironomid samples on the first axis of a PCA performed with square-root-transformed percentage data is shown.

Figure 5 Selected percentage curves of pollen, NPPs and chironomid taxa as indicators for regional vegetation change, lake ecology and chironomid assemblage. Diagram plotted on sediment depth (cm) with a secondary scale (cal. yr. BP) plotted for comparison. The sedimentological profile is plotted to the left of the curves.

Figure 6 Chironomid inferred July air temperature (CI-T) reconstructions from Lake Uddelermeer with sample specific error estimates. Curves plotted on age (cal. yr. BP) with a secondary scale of sediment depth (cm) plotted for comparison. Warm (red) and cold (blue) periods for the period 2550 - 1140 cal. yr. BP are indicated; the part of the record which is not included in the reconstruction is shown in grey. To the right of the reconstruction, the distance of the fossil sample to the nearest modern analogues in the Norwegian/Alpine training set (squared chi^2-distance (sq.x^2d.): the vertical lines indicate the 2nd and 5th percentiles of all squared chi^2-distances in the Norwegian/Alpine training set and are defined here as 'no close' and 'no good' analogues respectively (after Birks et al. 1990); the goodness-of-fit of the fossil samples to temperature (squared residual distance; sq.res.d): the vertical lines indicate the 90th and 95th percentiles in residual distances of the modern samples to the first axis in a constrained CCA and are defined here as a ‘poor’ and ‘very poor’ fit respectively (e.g. Birks et al. 1990); and the cumulative percentage

(Frequency %) of fossil chironomids that are absent (%absent) from the modern calibration set are given

Figure 7 CI-T reconstructions for Lake Uddelermeer (this paper); Bigland Tarn (Barber et al. 2013) and Talkin Tarn (Langdon et al. 2004) plotted on a cal. yr. BP timescale. Calibrated AMS radiocarbon dates and their 2 sigma error ranges are plotted to the right of each temperature reconstruction.

Figure 8 Warm (red) and cold (blue) periods in NW European temperature reconstructions for the period 1000 - 2500 cal. yr. BP (grey is not identified/available). IA: Iron Age; RWP: Roman Warm Period; DACP: Dark Age Cold Period; MCA: Medieval Climate Anomaly. A: CI-July air temperature Uddelermeer (this paper); B: CI-July air temperature Bigland tarn UK(Barber et al. 2013) also included in overview record D; C:Tree ring inferred JJA temperature for the Alps (Büntgen et al. 2011) also included in overview records D, E and F; D:Compilation various archives from NW Europe summer - winter and annual temperature (Riechelmann and Gouw-Bouman 2019); E:Compilation various archives N Hemisphere summer - winter - annual temperature (Ljungqvist 2009); F: compilation various archives globally temperature (Helama et al. 2017a). For the records A and C zone boundaries were placed where the temperature curve crossed the mean. When available, age uncertainty (minimum and maximum of the age model) is plotted with black lines.